THESIS FOR THE DEGREE OF DOCTOR OF PHILOSOPHY

SPATIAL ANALYSIS OF LIPIDS IN TISSUE SAMPLES APPLYING MASS SPECTROMETRY IMAGING

Masoumeh Dowlatshahi Pour

Department of Chemistry and Chemical Engineering
Chalmers University of Technology
Gothenburg, Sweden

2018

SPATIAL ANALYSIS OF LIPIDS IN TISSUE SAMPLES APPLYING MASS SPECTROMETRY IMAGING

Masoumeh Dowlatshahi Pour

ISBN: 978-91-7597-690-7

Doktorsavhandlingar vid Chalmers tekniska högskola
Ny serie nr 4371
ISSN 0346-718X

Department of Chemistry and Chemical Engineering
Division of Chemistry and Biochemistry
Analytical Chemistry
Chalmers University of Technology
SE-412 96 Gothenburg
Sweden
Telephone: +46 (0)31 772 1000

Front cover*:* A simple illustration of ionization process in SIMS imaging to produce ion images from a mouse brain tissue sample showing the distribution of phosphatidylcholine at *m/z* 184 (left) and cholesterol at *m/z* 369 (right) in the grey matter and white matter respectively.

Printed by Chalmers Reproservice
Gothenburg, Sweden 2018

Masoumeh Dowlatshahi Pour
Department of Chemistry and Chemical Engineering, Chalmers University of Technology

Abstract

Lipids are important naturally occurring components in all living cellular organisms. They serve as the main building blocks of cellular membranes, participate in many signaling pathways and are also stored as an energy source. Due to the extreme complex cellular chemistry and structure of lipids, there is a real need to have a label-free technique with high chemical specificity, high accuracy and high sensitivity for study of lipids within the cell membrane. Mass spectrometry imaging (MSI) is capable of providing information on the chemical composition and spatial distribution of complex biological molecules. MSI is a powerful label-free tool for lipid analysis across biological materials. Both matrix-assisted laser desorption/ionization (MALDI) and secondary ion mass spectrometry (SIMS), the two most common MSI techniques, have recently undergone many developments to improve spatial resolution and provide high sensitivity, mainly for higher mass species. These two techniques offer different capabilities in the analysis of a biological system. The main differences are that larger molecules can be ionized and detected using MALDI, whereas SIMS is capable of detecting mainly small molecules but at higher spatial resolution compared to MALDI. This thesis mainly focuses on two scopes of investigation with different sample modifications and also on the overall applicability of MSI for analysis of tissue samples. In recent years, some surface modifications have been developed to enhance the yield of intact molecular species in SIMS. One of them is matrix enhancement secondary ion mass spectrometry (ME-SIMS), which is the combination of the protocol for MALDI sample preparation and normal SIMS. In paper I, the possible mechanism of the signal enhancement in ME-SIMS was studied. Here, sublimation was used to deposit a thin layer of an organic matrix on the surface of a brain tissue slice analyzed with SIMS. In this work, I showed that sublimation could successfully provide enhancement in ion yields for a multitude of lipid species in SIMS. The mechanism of this enhancement could be due to a lower ion suppression followed by removal of the cholesterol crystals from the surface of sample allowing detection for less abundant species. It is also possible that the extraction of some specific lipids into the deposited matrix directly leads to an increase of higher mass lipid ion yield. In paper II, two different surface modifications, including matrix sublimation and nanoparticle deposition were applied on Drosophila brain samples and lipid information obtained from MALDI analysis were compared. Here, it was shown that each technique can be used in a complementary approach to detect a variety of lipid species. In paper III, SIMS imaging was employed to investigate the effect of specially processed cereals, as a specific diet on the alteration of lipid composition across the rodent intestine tissue. In paper IV, I continued the study of changes in lipid content, this time on brain samples of animals exposed to the same diet. Intake of such cereals increases active antisecretory factor (AF) in plasma, an endogenous protein with proven regulatory function on inflammation and fluid secretion. Although, the exact mechanism for the activation process of AF at the cellular level remains unclear. The results show changes in lipid content of cell membrane in response to this cereals intake suggesting a relation to activating AF. In paper V, the techniques for developing of sample preparation in SIMS imaging were investigated to improve the signal intensity of intact molecules at higher resolution.

Keywords*:* *Mass spectrometry imaging, SIMS, ME-SIMS, MALDI, Sample preparation, Lipid.*

List of publications

The thesis is based on the work contained in the following papers:

I. **An investigation on the mechanism of sublimed DHB matrix on molecular ion yields in SIMS imaging of brain tissue.**

Masoumeh Dowlatshahi Pour, Per Malmberg, and Andrew G. Ewing, *Anal Bioanal Chem., 2016 May, 408, pp 3071–3081.*

II. **Laser Desorption Ionization Mass Spectrometry Imaging of Drosophila Brain Using Matrix Sublimation versus Modification with Nanoparticles.**

Nhu T. N. Phan, Amir Saeid Mohammadi, Masoumeh Dowlatshahi Pour and Andrew G. Ewing, *Anal. Chem., 2016 Feb,* 88 *(3), pp 1734–1741.*

III. **Mass spectrometric profiling of lipids in intestinal tissue from rats fed cereals processed for medical conditions.**

Masoumeh Dowlatshahi Pour, Eva Jennische, Stefan Lange, Andrew G. Ewing and Per Malmberg, *Biointerphases, 2016 Jun, 11(2), pp 02A3101- 02A3107.*

IV. **Food induced changes of lipids in rat neuronal tissue visualized by ToF SIMS imaging.**

Masoumeh Dowlatshahi Pour, Eva Jennische, Stefan Lange, Andrew G. Ewing and Per Malmberg, *Sci Rep., 2016 Sep, 6, pp 327971- 327979.*

V. **Improved molecular imaging in rodent brain with time of flight secondary ion mass spectrometry using gas cluster ion beams and reactive vapor exposure.**

Tina B. Angerer, Masoumeh Dowlatshahi Pour, Per Malmberg, and John S. Fletcher, *Anal Chem., 2015 Apr, 87(8), pp 4305-4313.*

Related publications not included in the thesis

Zinc Regulates Chemical-Transmitter Storage in Nanometer Vesicles and Exocytosis Dynamics as Measured by Amperometry

Lin Ren, Masoumeh Dowlatshahi Pour, Soodabeh Majdi, Xianchan Li, Per Malmberg, and Andrew G. Ewing, *Angew. Chem., Int. Ed. 2017, 56, pp 4970 –4975.*

New frontiers in investigation of Psoriasis skin tissue by lable-free multi-modal imaging: a pilot study on phototherapy treated patient

Nisha Rani Agarwal[¥], Masoumeh Dowlatshahi Pour[¥], Maria Siekkeri Vandikas, Annika Enejder, Amra Osmancevic, Per Malmberg, *(Submitted).*

Imaging mass spectrometry as a novel approach to measure hippocampal zinc.

Masoumeh Dowlatshahi Pour, Lin Ren, Andrew G Ewing and Per Malmberg, *(Manuscript).*

Zinc Changes Lipid Composition of Cells and Mediates Plasticity in Exocytosis: Combining ToF SIMS with Electrochemical Quantification

Lin Ren[¥], Masoumeh Dowlatshahi Pour[¥], Per Malmberg and Andrew G Ewing, *(Manuscript).*

¥ Authors share first authorship with equal contribution to the paper.

Contribution report

Paper I. I took part in planning and designing the project with co-authors. I performed the experimental part and discussed the experimental issues with Per Malmberg and Andrew G. Ewing. I was responsible for analyzing and interpreting the data, and writing the first draft of the manuscript and responding to reviewer comments in consultation with other authors.

Paper II. I took part in planning and designing the project with co-authors. I assisted with sample preparation using sublimation for MALDI analysis. I contributed in writing part of the manuscript.

Paper III. I took part in planning and designing the project with co-authors. I performed and contributed to experiments, data analysis, and interpretation. I wrote the majority of the first draft of the manuscript and responded to reviewer comments in consultation with co-authors.

Paper IV. I took part in planning and designing the project with co-authors. I performed and contributed to experiments, data analysis, and interpretation. I wrote the majority of the first draft of the manuscript and responded to reviewer comments in consultation with co-authors.

Paper V. I took part in experimental part with Tina B. Angerer and contributed in performing sample preparation, data analysis, and interpretation. I contributed in writing part of the manuscript.

List of abbreviations

AA – Arachidonic acid

AF – Antisecretory factor

AuNP – Gold nanopartilces

CHCA – α-cyano-4-hydroxycinnamic acid

DAG – Diacylglycerol

DHB – Dihydroxybenzoic acid

FA – Fatty acid

GCIB – Gas cluster ion beam

ITO – Indium tin oxide

LDI – Laser desorption ionization

LMIG – Liquid metal ion gun

MALDI – Matrix-assisted laser desorption ionization

ME-SIMS – Matrix-enhanced secondary ion mass spectrometry

MetA-SIMS – Metal-assisted secondary ion mass spectrometry

MSI – Mass spectrometry imaging

NP – Nanoparticle

OPLS-DA – Orthogonal partial least squares discriminant analysis

PC – Phosphatidylcholine

PE – Phosphatidylethanolamine

PG – Phosphatidylglycerol

PI – Phosphatidyinositol

PS – Phosphatidylserines

SALDI – Surface assisted laser desorption ionization

SEM – Secondary electron microscopy

SIMS – Secondary ion mass spectrometry

SM – Sphingomyelin

SPC – Specially processed cereals

TAG – Triacylglycerides

TFA – Trifluoroacetic acid

ToF –Time of flight

UHV – Ultra-high vacuum

Contents

1. The Brain and Neuronal Communication

The human brain is one of the main parts of the central nervous system (CNS). It is the most complex organ, which controls biological processes in the human system, from simple bio-processes in single cells to complicated processes in complex organs. In fact, the brain is involved in a wide range of specific body functions, including motor control and physical motions, hormone regulation, cognition processes, thought, perception, emotion and many other biological activities and processes. The brain comprises two main groups of cells including nerve cells (neurons) and support cells (glia cells) [1,2] which are described in detail in following sections in this chapter.

1.1 Neurons

Due to the massive variety of brain-controlled processes, the brain necessarily links and communicates with the whole body through a very complicated communication system called the neuronal network. The human brain has been estimated to consist of a billion neurons which are responsible for cellular communication, signaling and transition of information within the network. Neurons can communicate with each other via a junction called a synapse, which is a region about 12-20 nm between two adjacent neurons [3,4] Figure 1.1 shows a schematic of a neuron and the synaptic connection between two neurons. Compared to the other cell types of the body, neurons are structurally different. They are polarized and typically composed of dendrites, a cell body, and an axon with the axon terminals.. Each of these possesses a specific function.[5,6]

The cell body (soma or perikaryon) comprises the nucleus and also some other intracellular organelles containing microtubules, ribosomes, golgi, mitochondria, and exclusively neurofilaments which are essential for cell functioning. The dendrites are short processes that extend from the cell body and they are generally divided into smaller branches. The function of the dendrites is to receive signals and information from neighbouring neurons in the synaptic space and then carry signals to the cell body. And at the cell body, small electrical impulses are formed from chemical signals received from presynaptic neurons. These small impulses are then integrated forming a larger potential called an action potential, which

travels along the axons and allows the neuron to transmit electrical signals over some distance. Axons are long extensions projecting from the cell body to transfer neuronal outputs typically to dendrites of adjacent neurons via a synaptic junction.[1,2]

To help better conduction of the action potential, the axons are periodically covered by a thick non-conductive layer composed of lipid substances called the myelin sheath. The process of adding and accumulation of myelin on the axon is called myelination, which is performed by glial cells. The electrically insulating myelin sheaths wrapped around the axon allow transmission of the action potential along the nervous system at considerably higher speeds.[2,7]

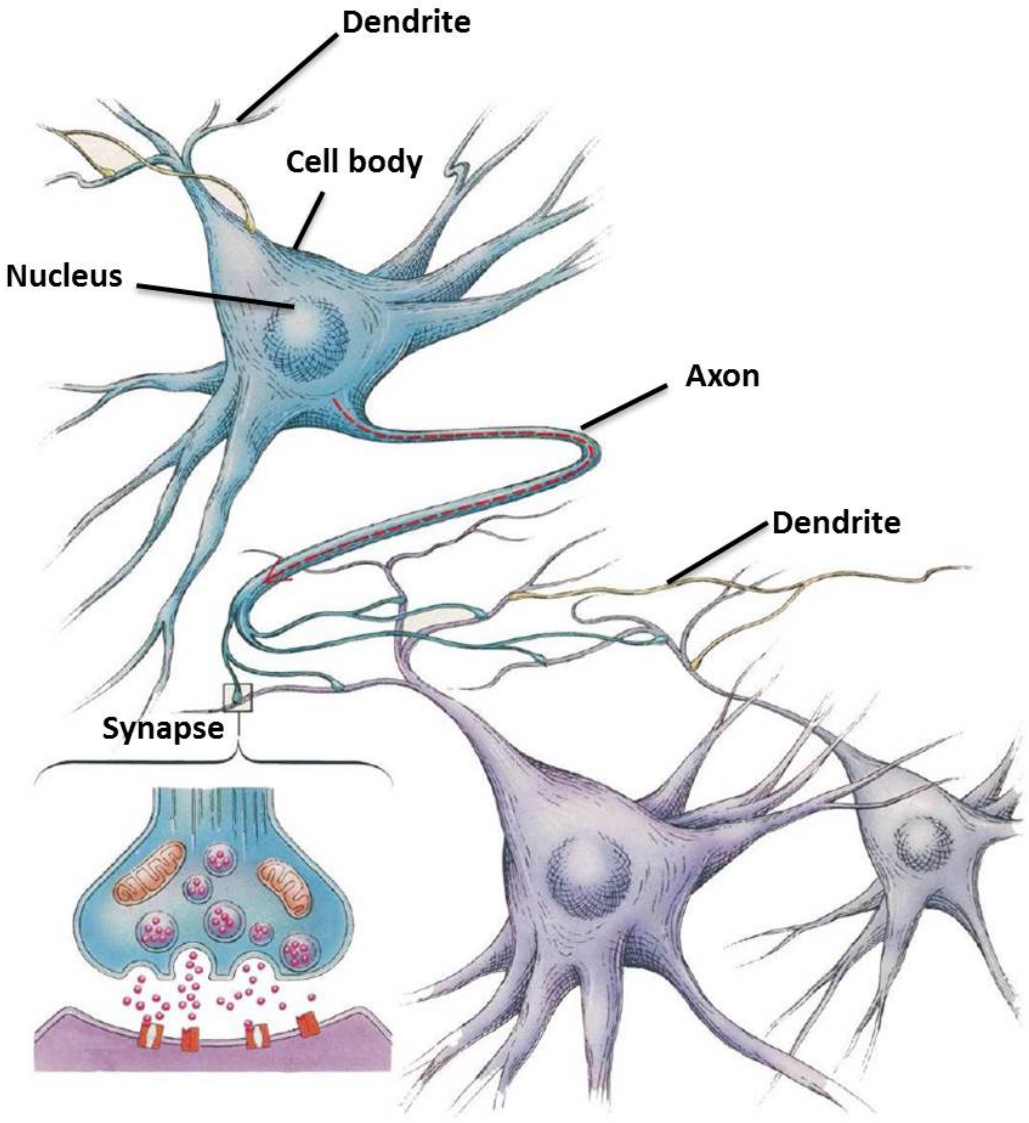

Figure 1.1 An illustration of neuronal structure. Neurons contain 3 main parts; the cell body, the dendrites and the axon. Neurons are typically connected to each other through a structure called a synapse where cellular communication occurs either electrically or chemically. Image reproduced with permission from Fischbach.[8]

Neurons differ in many ways based on their morphology and function. Also, based on polarity, neurons are placed in three different categories of unipolar, bipolar and multipolar (Figure 1.2). In this regard, neurons can be recognized as unipolar when the axon and dendrites grow from the same place on the cell body. Neurons are considered bipolar when a single dendrite and the axon branch from opposite sides of the cell body. If neurons contain one axon with multiple dendrites allowing them to receive signals from other neurons via multiple synaptic points, they are considered multipolar.[1,2,7]

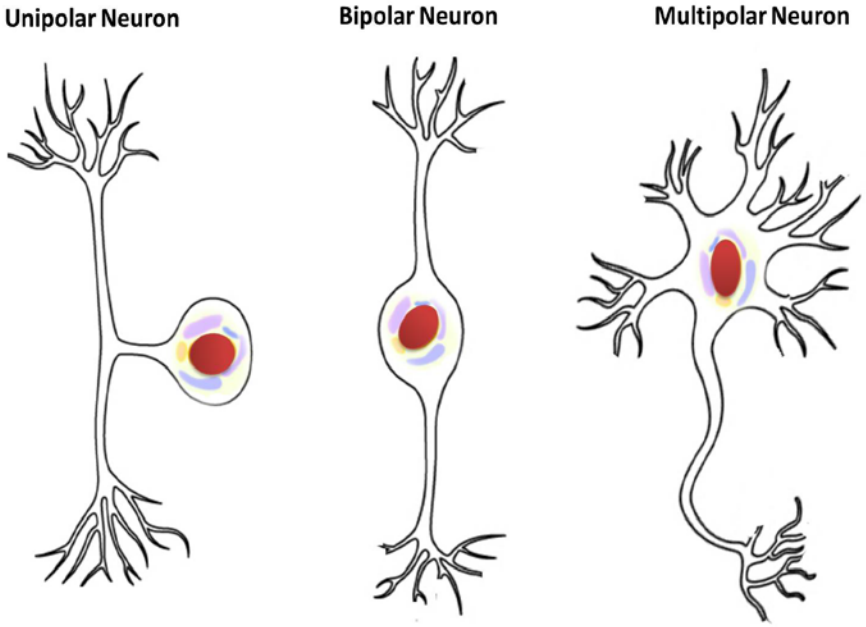

Figure 1.2 Schematic for structures of three different classes of neurons based on their polarity: unipolar, bipolar and multipolar.

1.2 Glial cells

Another abundant cell type in the brain is the neuroglial cells, which are 10 times more abundant than neurons and indeed compose the bulk of the nervous system. Glial cells have been recognized in two main categories of macroglia and microglia. Macroglia in turn consists of three different classes; 1. oligodendroglia cells, which serve to form myelin sheets around the axon in the central nervous system (CNS); 2. ependyma cells that make myelin sheets in the peripheral nervous system (PNS); and 3. astrocytes play crucial roles such as

providing the neurons with nutrients by releasing growth factors, supporting the structure of the nervous system, improving the efficiency of cell signaling between the neurons and also aiding neuronal migration. Microglia cells act as an important agent in the destruction of pathogens and removal of dead neurons.[7]

Moreover, as glial cells are key factors in maintaining the proper functioning of nervous system, significant alteration in their function can be observed in disorders and diseases such as Parkinson's disease (PD), Alzheimer's disease (AD) and Amyotrophic lateral sclerosis (ALS).[9]

1.3. Grey and white matter in the brain

In general, there are two different kinds of tissue in the CNS, grey and white matter. The grey matter, which appears as gray in color is largely comprised of cell bodies, dendrites, and axonal terminal of neurons. Typically, synaptic communication between neurons mostly occurs in this region. White matter, which is referred to as the area with an off-white colour, mainly contains myelinated axons and in this area, neuronal signals are transmitted via axons over long distances.[2]

1.4 Animal models for biological studies

1.4.1 The rodent nervous system

There are common similarities known between rodents, particularly rats and mice, and human beings in terms of mammalian genes and biochemical pathways. More importantly, both rodents and humans suffer from many of the same diseases due to having the same basic physiology, organs, and body plans. In recent years, genetic engineering has produced rodent models of disease for clinical, behavioral, and physiological investigations. A remarkable variety of studies using rat models have been presented to characterize the causes of neurological diseases, to find insights into neuronal mechanisms, and also to assess potential drugs and new therapeutic options for humans.[10-12]

A detailed anatomic and structural study of the rat brain has been comprehensively done by Tsujino and Sakurai.[13] Figure 1.3 depicts anatomy and structure of different regions in a sagittal section of the rat brain.

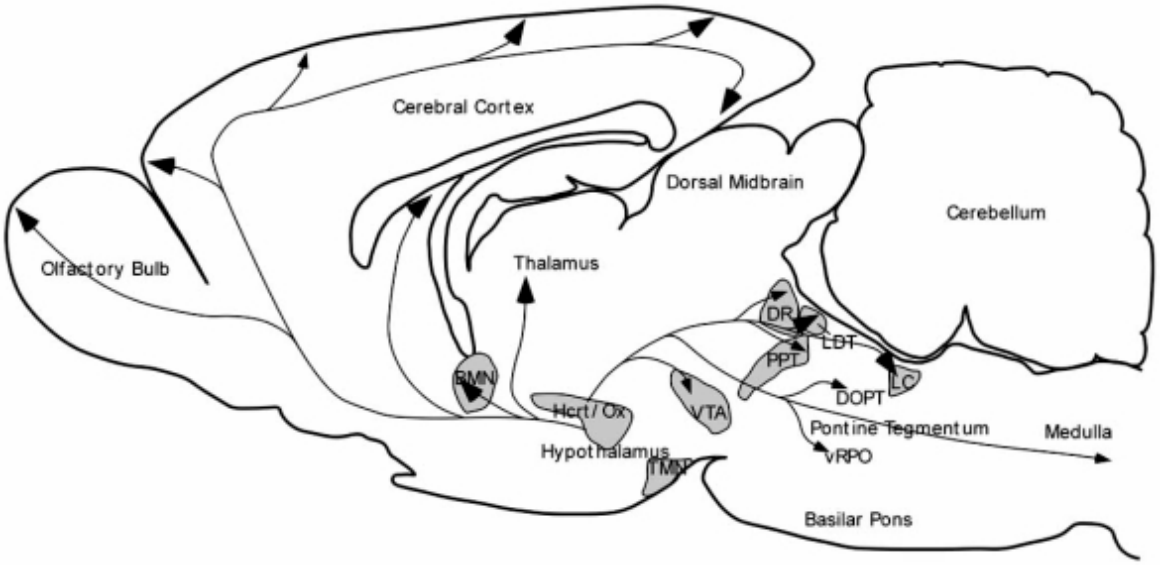

Figure 1.3 Schematic illustration of a sagittal section displaying the main parts of the rat brain. Image reproduced with permission from Nuñez et al.[14]

1.4.1.1 Cerebellum region and functions

The main tissue type used in this thesis is rat brain cerebellum. The cerebellum is also called the little brain as it is found in the posterior brain hemispheres, located above the brainstem; the structure which forms the connection between spinal cord and brain. The cerebellum makes up about 10 percent of the total weight of the brain, and it has a symmetrical structure with two hemispheres surrounded by cerebellar cortex which is made up of grey matter. The cerebral cortex in the cerebellum is the outermost layer which is composed of neurons densely folded to pack as much surface area as possible into the small space. The cerebellum contains roughly about half of the total number of neurons within the entire mammalian brain. [15,16]

Figure 1.4**a**, shows a dorsal view of the cerebellum of a rat brain depicting its geometrical structure which contains three divisions of one midline vermis as the major axis in the middle of two lateral hemispheres positioned at each side. A sagittal slice of the rat cerebellum, illustrated in Figure1.4**b,** indicates ten various lobules of the cerebellar cortex making up the entire structure of cerebellar region. The cortical layer in each lobule basically consists of three different layers with the molecular layer (ML) as the outermost layer, the Purkinje Perikarya layer (PL) located in the middle and the bottom layer which is called the Granule Cell (GL) layer (Figure 1.4**c**). Also, a thin sheet of white matter can be seen in the middle of the structure.[17]

The cerebellum is involved in a variety of functions related to body movement and coordination such as maintaining balance, posture, and gait. [18,19] Also, some recent evidence has been found to implicate the involvement of the cerebellum in a wide range of non-motor higher cognitive functions[20] including language,[21] planning and prediction,[22] learning, emotional memory and emotional experience,[23-27] sex and orgasm,[28,29] and perceptual ability.[30]

In addition, dysfunction of the cerebellum has been reported to be involved in some disorders including Bipolar disorder, Schizophrenia, and Specific Language Impairment.[31-33]

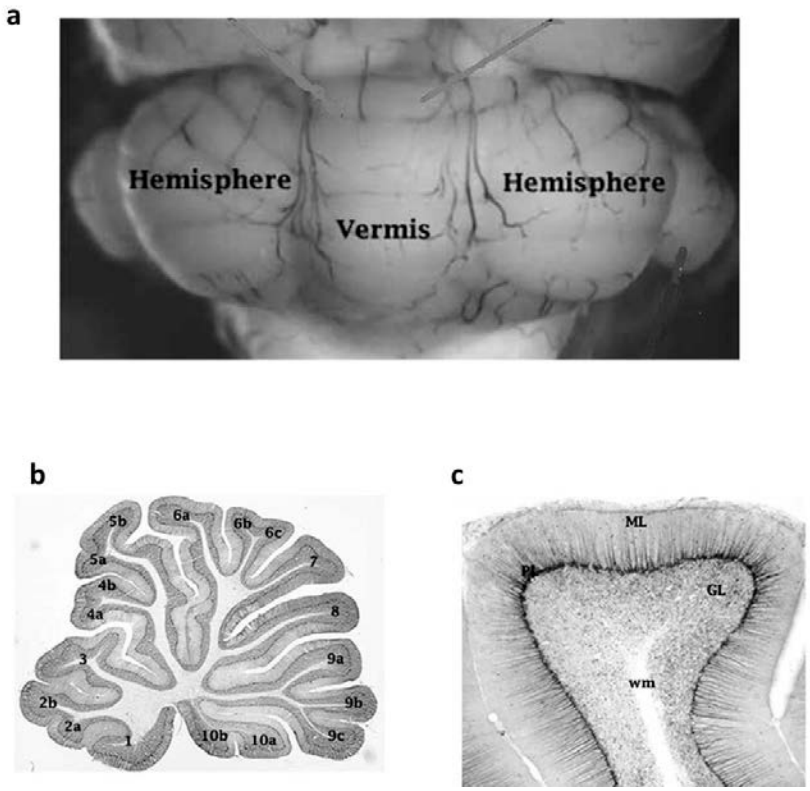

Figure 1.4 The ret cerebellum. **a**: An illustration from dorsal view of the cerebellum in the rat brain. The structure shows an ellipse with a central area called the vermis surrounded by two lateral hemispheres. **b**: A sagittal cross-section of the rat cerebellum showing 10 different lobules in the structure of the cerebellar cortex. **c**: An expanded view of Lobule 7 illustrating three different layers of cerebellar cortex: Molecular Layer (ML) as the outermost layer, Purkinje Perikarya Layer (PL) located in the middle and the bottom layer which is called the Granule Cell (GL) layer (Figure 1.4 c). Also, a thin sheet of white matter is filled in the middle of the structure cortical. Image reproduced with permission from Miquel and et al.[17]

1.4.2 Drosophila melanogaster brain

Drosophila melanogaster (fruit fly) is known as an ideal model organism in biological studies with many advantages.[34-37] Flies reproduce fast (around 100 eggs per day), which is very advantageous for large population studies, statistical analysis, and genetic experiments requiring different generations. In this model, molecular mechanisms such as metabolism, organogenesis, and also neural development have been found to be comparable to humans and mammals. In addition, the fly possesses a variable range of behavioral patterns including learning and memory, sleeping, stress, aggression, drug addiction, and alcohol tolerance, which all imply the existence of refined and developed motor systems, cognitive processes, and coordinated sensory inputs. The nervous system of the fly is very similar to the nervous

systems of mammals, particularly the neurotransmitter system and neurological functions related to different parts of the brain.[38-40] The *Drosophila* brain is small, with a volume about 5 nL, and contains more than 100 000 neuronal cells forming complex nervous circuits to carry out a variety of higher order neurological processes.[40]

Figure 1.5 depicts a view from the structure of the adult head of *Drosophila melanogaster* (**a**) and also a colored schematic of the fly brain showing the main regions and related structures (**b**).

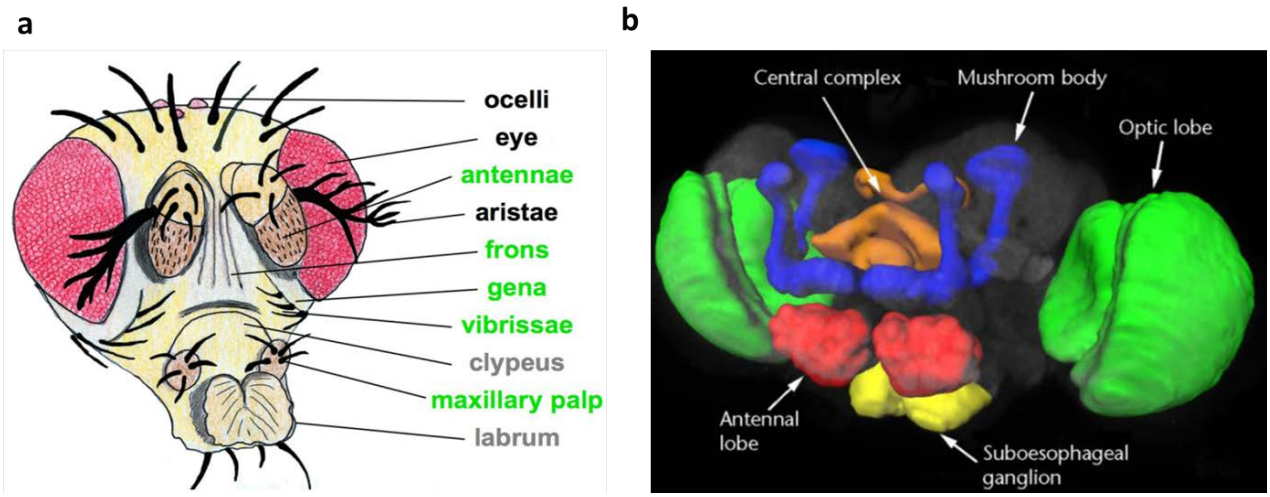

Figure 1.5 The fly head and brain. **a:** Drawing of the adult head of *Drosophila melanogaster* showing different related parts. Image reproduced with permission from Atkins et al.[41] **b:** Color-coded representation of the main regions of the fly brain. Image reproduced with permission from Heisenberg et al. [42]

As can be seen in Figure 1.5**b**, the *Drosophila* brain contains of two main parts, the central brain and the optical lobes. The central brain, the so-called protocerebrum, mainly consists of several regions facilitating different neurological processes. The essential region is the mushroom body which is located in the dorsal and posterior portions of the central brain. The mushroom body region is a center of learning, memory, and olfactory as well as multisensory functions processing. Another part is the central complex, a structure found along the midline of the central brain, which serves a key role in connecting many parts in the central brain and is also involved in integrating and guiding behavior and activities, particularly motor, locomotion, sensory, learning, and memory functions.[43,44]

The antennal lobes region is another part of the central brain, which is placed in the anterior area and forms the primary olfactory center in *Drosophila*. The lobes possess the olfactory receptor neurons that are essential for the flies to detect odor and identify food and distinguish their partners and predators.[45] These lobes are connected to each other and also to the mushroom body as well as other parts of the brain by several kinds of neurons including local neurons, projection neurons, and centrifugal neurons. The final region is the suboesophageal ganglia, a region in the central brain which is associated with regulation of gustatory neuron activities.[46] The optical lobes region contains about 60 000 neurons on each side and is another part of the fly brain which is responsible for vision activities.[47]

In this thesis, the brain tissue sections from both rat and fruit fly models have been successfully used to demonstrate as proof of principle the methods, but also to study new neuroscience. These models will be further discussed for the experimental analysis with greater details later in this thesis.

2. Lipids and Biological Functions of Lipids

Lipids are small naturally occurring molecules in all living organisms. As they have a hydrophilic polar head group and hydrophobic nonpolar tails in their structure, all lipid molecules in the cell membrane are naturally amphipathic.[48] Lipids play different critical functions in biological systems. The key function of lipids is the formation of lipid bilayers in the cell membrane (Figure 2.1). Here the lipids provide the structural integrity required for protein function as well as serving as lipid anchors to bind proteins to the cell membrane. Also, lipids are involved in signaling pathways acting as secondary messengers in signal transduction and synaptic transmission. Furthermore, lipids are well-known energy storage molecules, particularly in the form of fatty acids (FA) and triacylglycerols (TAG). Another function of lipids is to serve as vitamins and hormones.[49,50]

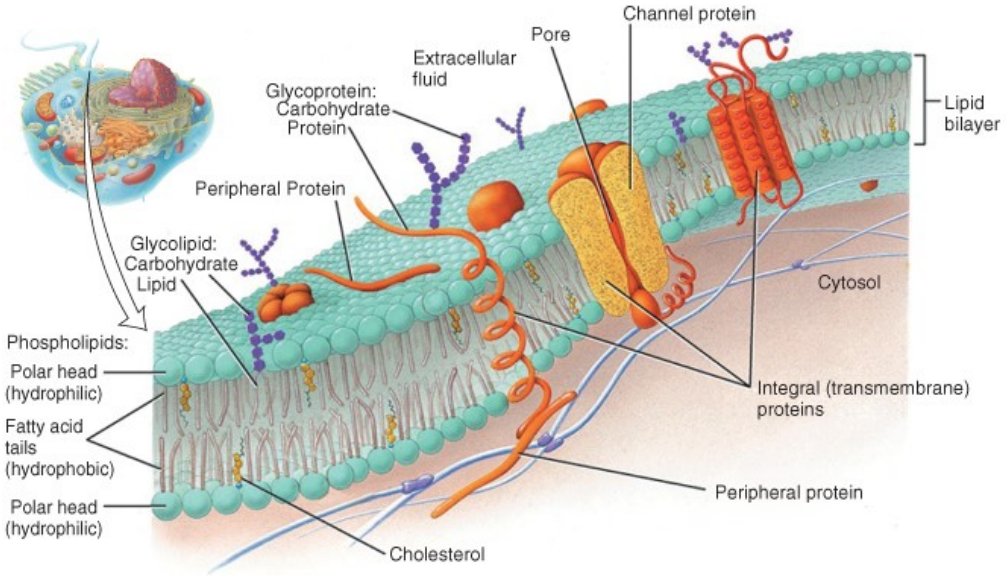

Figure 2.1 Schematic representation of the cell plasma membrane illustrating different chemical constituents containing lipids as the main structure of the membrane. Image reproduced with permission from Marieb et al. [51]

2.1 Categories of lipids

Lipids differ considerably in structure and chemical properties. Different biochemical transformations and pathways can make the lipid structures more complex during their biosynthesis. Due to this level of diversity, a comprehensive classification and chemical

representation system is required to properly cover the broad range of lipids. Accordingly, a number of classification systems have been developed which classify lipids by different characteristics, such as polarity, solubility or degree of saturation. A comprehensive classification system for lipids was published in 2005 by Fahy et al. to establish a universal nomenclature for lipids.[52] From this, biological lipids are defined as amphipathic small molecules that are originally made of two biochemical subunits: ketoacyl groups and isoprene groups (Figure 2.2). Using this approach, lipids can be classified into eight different groups: sphingolipids, saccharolipids, fatty acyls, glycerolipids, glycerophospholipids, polyketides, prenol lipids, and sterol lipids. This lipid classification includes almost all subgroups of lipids; however, only the lipid groups that are abundant in brain tissues will be discussed here.

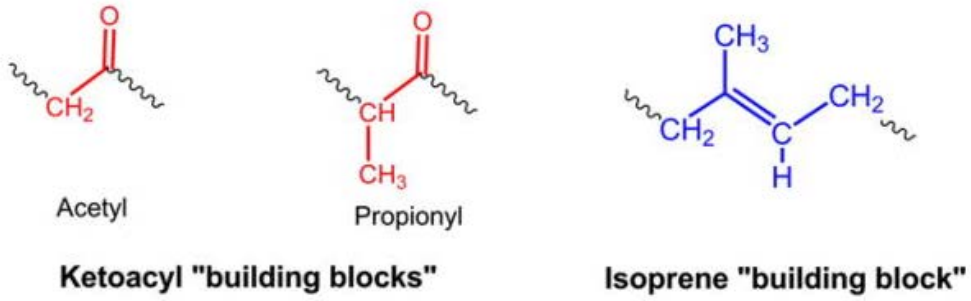

Figure 2.2 Lipid building blocks. The LIPID MAPS classification system is based on two fundamental biosynthetic concepts "building blocks": isoprene and ketoacyl groups. Image reproduced with permission from Fahy et al.[52]

2.1.1 Fatty acyls

Fatty acyl is a general name for describing fatty acids, their conjugates, and derivatives. The fatty acid as one of the most fundamental classes of biological lipids is essentially made of a terminal carboxylic acid with a long saturated or unsaturated aliphatic chain. The fatty acid structure is commonly used as a building block of complex lipids. Since they are commonly being formed from two carbon acetyl-CoA molecule extensions, most naturally occurring fatty acids are straight-chain carboxylic acids with an even number of carbon atoms. However, odd-chained and branched fatty acids have also been found, for instance in protozoa and bacteria.[53] Fatty acids exist as either free fatty acid (FFA) molecules or fatty acyl esters in more complex lipid components such as phospholipids, diglycerides, and triglycerides in the body. The majority of the fatty acids found in lipids are monocarboxylic acids.[54]

2.1.2 Glycerophospholipids

The glycerophospholipids are abundant in nature and are key components of the lipid bilayer of cells. Glycerophospholipids, which are glycero-containing lipids can be considered to be glycerolipids, but due to their abundance and importance, they are placed in a separate category. Glycerophospholipids, with an amphiphilic structure, are essentially formed from 2 fatty acid tails as the nonpolar part of the lipid, connected to a polar head-group which contains a phosphate group esterified to a glycerol backbone (Figure 2.3). Depending on the polar head group structure, different subgroups with different biological functions are defined for the lipids in this category. Correspondingly, the main subclasses are phosphatidylcholine (PC), phosphatidylethanolamines (PE), phosphatidylserines (PS), phosphatidylinositols (PI), and phosphatidylglycerol (PG). Among them, the most abundant phospholipids in the brain are PE, PC and PS and the amount and distribution of these lipids vary significantly within specific brain regions.[55,56]

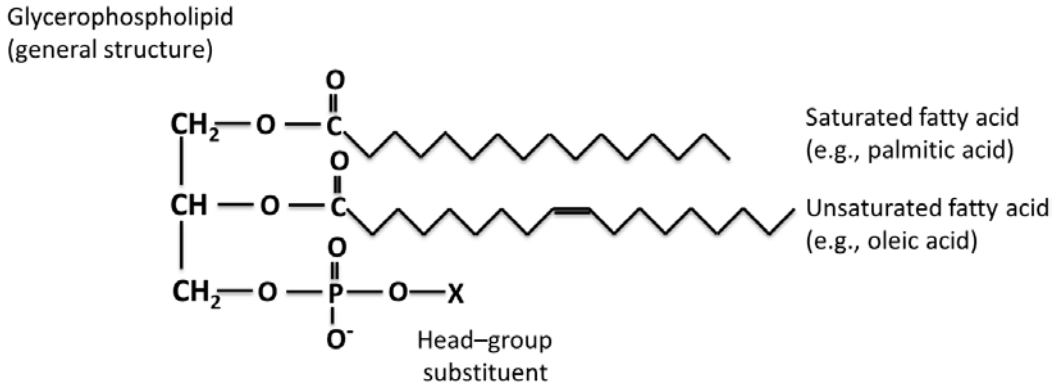

Figure 2.3 General structure of glycerophospholipids displaying the polar head group and hydrophobic tail.

2.1.2.1 Phosphatidylcholine (PC)

Phosphatidylcholines (PCs) (Figure 2.4) are the most abundant lipid species in the class of glycerophospholipids and incorporate choline as a head-group. They are the major constituents in the lipid bilayer of cell membranes, specifically in brain tissue. PCs with head and tail groups of approximately the same size are lamellar in (cylindrical) shape, and as such are dominantly distributed in the outer leaflet of cell membranes.[57] Since the choline head-group contains nitrogen in its structure, PC molecules can be either net neutral in charge as zwitterions with a positive amine combined with a negative phosphate group, or gain a positive charge by protonation in mass spectrometry.[58]

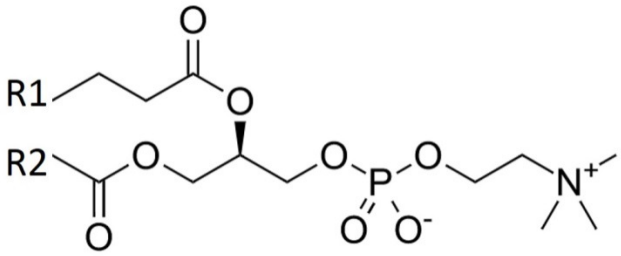

Figure 2.4 Typical molecular structure of phosphatidylcholines comprised of a glycerophosphoric acid and a choline head group, with various kinds of fatty acids (R1 and R2 that can be saturated or unsaturated).

2.1.2.2 Phosphatidylethanolamine (PE)

Phosphatidylethanolamine (PE) (Figure 2.5) covering about 15–25% of the total lipid content in mammalian cells is the second most abundant phospholipid after PC. The main building block to form PE is ethanolamine (H_2N-CH_2-CH_2-OH), which occurs in every cell in the human body as the head group of PE. Owing to a small head group compared to its hydrophobic tails, PE has a conical shape causing curvature properties to the cell membrane. PE is therefore enriched in the inner leaflet of membranes and as a zwitterionic molecule is able to yield both positive and negative molecular ion species in mass spectrometry.[59,60]

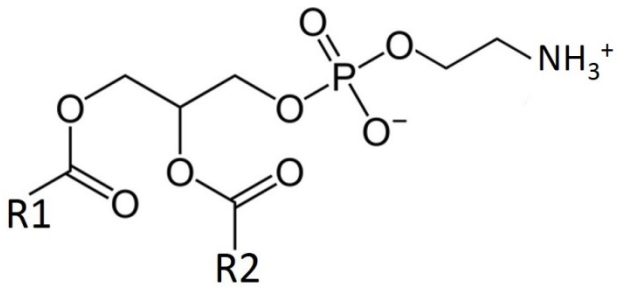

Figure 2.5 General structural formula of phosphatidylethanolamine displaying a combination of glycerol esterified with two fatty acids and phosphate group that are linked to an ethanolamine group.

2.1.2.3 Phosphatidylserine (PS)

Phosphatidylserine (PS) is another lipid in the glycerophospholipid category. It consists of two fatty acids linked to an ester connection to the first and second carbon of glycerol and serine. The serine molecule is attached through a phosphate group linkage to the third carbon of the glycerol lipid (Figure 2.6). Similar to other conical shaped lipids, it is mainly distributed in the inner leaflet of membranes. However, surface-exposed PS occurs during cell death or damage since PS is transported to the outer cell membrane on cells undergoing apoptosis.[61,62]

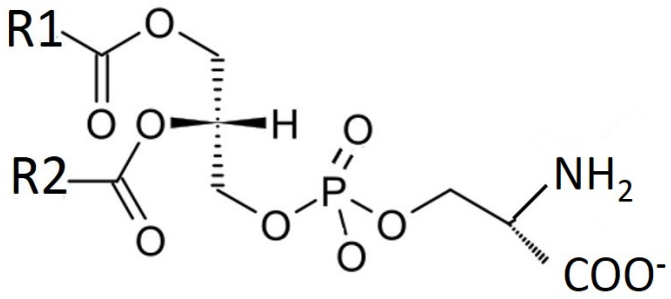

Figure 2.6 General structural formulation of phosphatidylserines presenting attachment of two fatty acids to the first and second carbon of glycerol backbone and serine which is attached through a phosphate group linkage to the third carbon of the glycerol lipid.

2.1.2.4 Phosphatidylinositol (PI)

Phosphatidylinositol (PI) is formed from a glycerol backbone, with an inositol ring and a phosphate at the sn−3 position and two acyl chains esterified at the sn−1 and sn−2 positions. The inositol ring can be phosphorylated at different places in which seven unique species known as phosphoinositides (PIPns) can be generated (Figure 2.7). PIs are well known as both signaling molecules and key structural constituents of the cell membrane in various eukaryotes. They can be found in all tissues; however, they are mostly present in the brain. Since PI has several OH groups on its head-group, it can easily carry a negative charge and be detected as $[M-H]^-$ species in ToF-SIMS.[63]

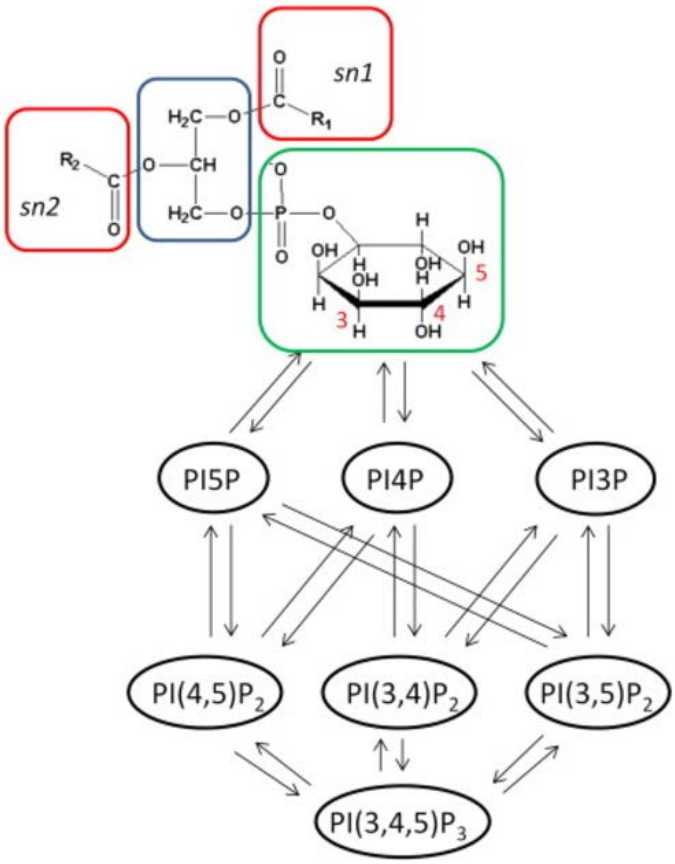

Figure 2.7 The structural formula, arrangement and also the production of phosphatidylinositol. Phosphatidylinositol is formed from a glycerol backbone (blue), two acyl chains at the sn−1 and sn−2 positions (red) and an inositol headgroup (green). The hydroxyl groups can be phosphorylated at positions 3, 4 and 5, generating seven typical phosphoinositide species. Image reproduced with permission from D'Souza et al.[63]

2.1.2.5 Phosphatidylglycerol (PG)

Phosphatidylglycerol (PG) as the simplest glycerophospholipid consists of a glycerol molecule in which the hydrogen of one of the primary hydroxy groups has been replaced by a phosphatidyl group (Figure 2.8). PG is the second most abundant lipid species in bacterial cell membranes. Also, it occurs in plant and in mammalian cells (mainly in mitochondria) but in low abundance.[64]

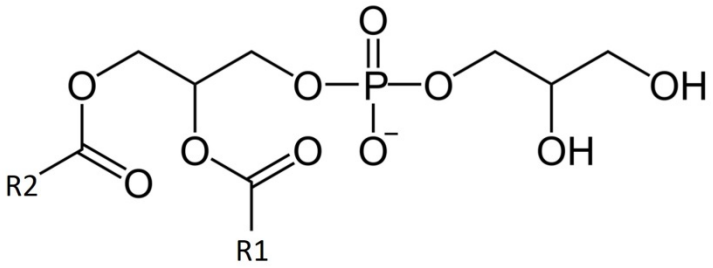

Figure 2.8 General chemical structure of a phosphatidylglycerol showing a phosphatidyl group which is replaced with the hydrogen of one of the primary hydroxy groups in glycerol molecule.

2.1.3 Sphingolipids

The amino group of sphingosine is acylated with long chain fatty acids and the N-acylated product is termed a ceramide, which is linked to different head groups to form various membrane lipids. Indeed, ceramide is a sphingolipid with an R group composed of only a single hydrogen atom. The R group comprising phosphocholine yields a sphingomyelin, and numbers of sugar monomers or dimers, yield cerebrosides and globosides, respectively (Figure 2.9). Contrary to the glycerophospholipids, simple sphingolipids with sufficiently amphipathic structure can freely diffuse and flip between the inner and outer leaflet of the cell membrane.[65]

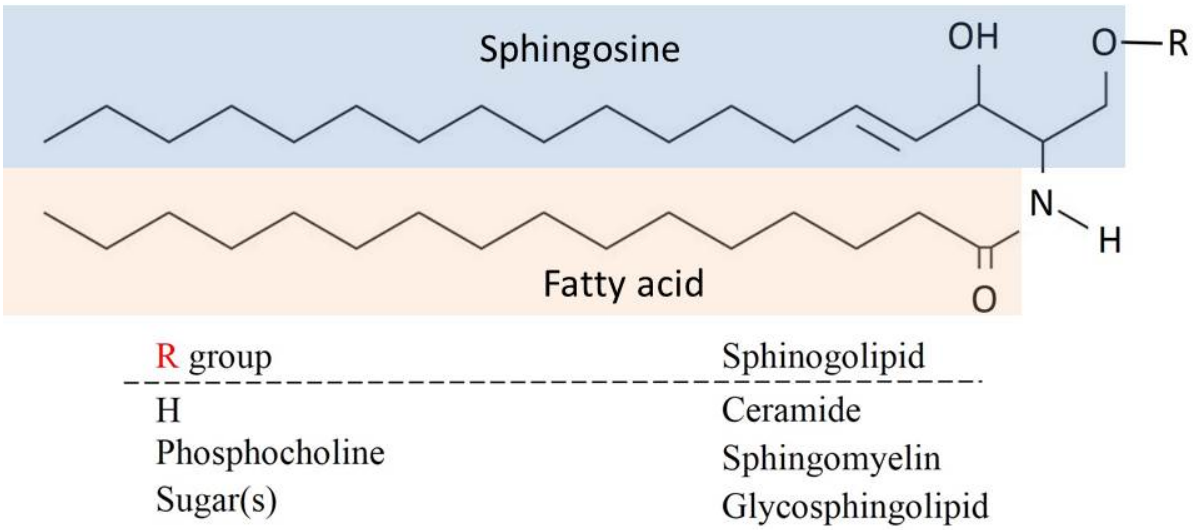

Figure 2.9 Structural representation of sphingolipids: contains a sphingosine, a long chain aliphatic amino alcohol, long chain fatty acid and different head groups (as R) yielding major classes of sphingolipids.

2.1.3.1 Sphingomyelin (SM)

Sphingomyelin (SM) is the most abundant complex type of sphingolipid found in mammalian cell membranes, especially in the membranous myelin sheath, which surrounds nerve cell axons. Among the membrane phospholipids in humans, sphingomyelin is the only one not derived from glycerol. Structurally, it is the phosphodiester of ceramide and choline, which is generated by a reaction that transfers the head group of PC to ceramide. [66,67]

Similar to PC, the choline head group makes it zwitterionic with no net charge; however, it is also capable to be ionized as a positively or negatively charged species by the loss of a methyl group.

2.1.3.2 Gangliosides

Gangliosides, as the most abundant lipids in the nervous system, are a varied group of lipids composed of a glycosphingolipid with one or more sialic acids linked to a sugar chain. These complex lipid species are generally characterized based on heterogeneity and diversity of the structures in their carbohydrate chains. Accordingly, 188 gangliosides with different carbohydrate structures have been identified so far. In cells, gangliosides are primarily localized in the outer leaflets of plasma membranes. The expression levels and patterns of brain gangliosides are considerably changed during brain development. For instance, simpler forms of gangliosides are present in developing brains, while more complex gangliosides are found in the adult brain.[68] Because of their acidic nature, they produce a negatively charged species in mass spectrometry.

2.1.4 Sterol lipids (cholesterol)

Sterol lipids have the unit structure of a five-carbon branched chain. The most abundant lipid component from this category in the brain is cholesterol (Figure 2.10), which is an essential structural component of animal cell membranes and is necessary for providing both the structural integrity and fluidity of the cell membrane. Cholesterol is capable of freely traveling between the inner and outer leaflet of the membrane. It plays a key role in the formation of lipid rafts and is responsible for protein trafficking and signaling at the cell surface.[69] In mass spectrometry, cholesterol can be ionized to $[M+H-H_2O]^+$ and to the negative species of $[M-H]^+$ but in lower abundance.

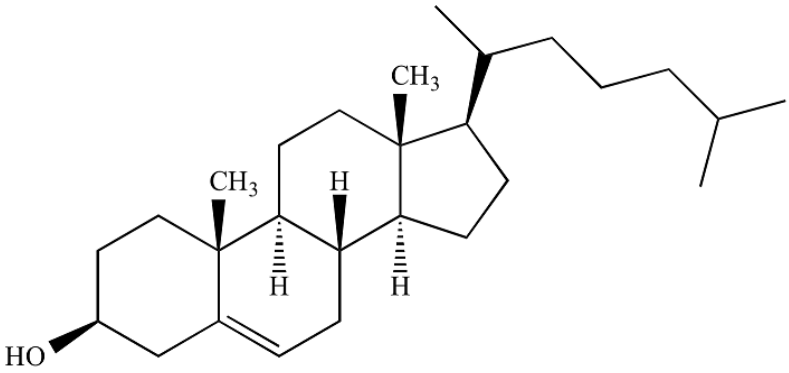

Figure 2.10 Representative structure of cholesterol (a combination of steroid and alcohol) with its polar hydroxyl group which can be esterified by a fatty acyl residue.

2.2 Biological functions of lipids

2.2.1 Lipids as the integral components of cell membranes

The plasma membrane creates the protective barrier surrounding all cells. The main constituents of the plasma membrane are lipids which provide an efficient shield against the aqueous environment owing to their hydrophobic and hydrophilic sections in their structures.[48] Notably, among different lipid groups, cholesterol and glycerophospholipids are the two main lipid components in the lipid bilayer of the cell membrane. Specifically, brain tissue mainly consists of three major categories of lipids; cholesterol, glycerophospholipids (phosphatidylcholine, phosphatidylethanolamine, and phosphatidylinositol) and sphingolipids (sphingomyelin, cerebrosides, sulfatides, and gangliosides) to such an extent that brain contains 20% of the body's total cholesterol and also 20-25% of brain's dry weight is composed of glycerophospholipids.[56,70]

In the cell membrane, lipids arranged in cholesterol and sphingolipid-rich microdomains are called lipid rafts. [71] These rafts are enriched with transmembrane proteins and ion channels. Lipid rafts have also been implicated to serve as protein anchors to attach proteins to the cell membrane and to aid regulate protein functions as well. Moreover, K^+ and Ca^+ channels functions are affected by lipids and fatty acids such as arachidonic acid a lipid-based second messenger.[49] This will be discussed in more details later in this section.

Lipid organization in the cell membrane can be associated with regulation of bioprocesses in cells such as exocytosis; the process of membrane fusion of an intracellular trafficking vesicle with the cellular membrane of the presynaptic neuron to release neurotransmitters. Lipid

composition and their geometry can play a regulatory role in the membrane fusion of the vesicle and the plasma membrane. In fact, glycerophospholipids based on their shape and geometry, rearrange their localization across the cell membrane during exocytosis. Such that the lamellar shaped lipids including PC and sphingomyelin are highly localized away from, whereas conically shaped lipids such as PI, PE and PS accumulate in the high curvature fusion pore site. These changes in lipid structure and distribution of various lipid compositions provide sufficient flexibility of the membrane during fusion process facilitating exocytosis.[57]

2.2.2. Lipids serve as an energy source

In general, fatty acids (FA) and triacylglycerols (TAG), are viewed as the main reservoirs of energy for biological systems. FAs and TAGs are efficiently reduced producing higher energy (38 kJ/g) than the other types of energy sources including carbohydrates and proteins (17kJ/g). In addition, since lipids have hydrophobic properties, they are stored in anhydrous forms which provide a highly concentrated energy source for biological reactions.[54]

2.2.3. Lipids as second messengers in cellular signaling

Lipids play the role of second messengers in many cellular signaling pathways via biosynthetic and metabolic reactions with different enzymes. Second messengers are generated via different complex catalytic mechanisms from different precursors in biological reactions. Also, there is in general a relation among biochemical reactions involved in this process and one single pathway can affect other related signaling pathways. Arachidonic acid (AA), a 20 carbon polyunsaturated fatty acid and one of the most important lipid-based second messengers is essentially produced via the hydrolysis of glycerophospholipids by phospholipase. AA is also generated from a serial metabolic process in which AA is produced by the hydrolysis of phosphatidylinositol 4,5-biphosphate to diacylglycerol (DAG) and subsequently, the hydrolysis of DAG by phospholipase C.[56,72] AA serves as modulating of Ca^{2+}, K^{+} ion channels and protein kinase C activities and also the monoamine transporters by inhibiting glutamate uptake.[57,73]

Diacylglycerols (DAGs), another major group of second messengers are generated by the catalytic cleavage of glycerophospholipids, mostly PI, PC, and PE. In addition, DAGs generally serve as precursors for second messengers such as PA and AA.[56]

Ceramides are metabolites, which are essentially generated from hydrolysis of sphingomyelin by sphingomyelinase. These lipid components have been implicated in several physiological cellular functions including cellular reaction to stress and injury, apoptosis, cell growth arrest, differentiation, cell senescence, cell migration and adhesion. Also, it has been shown that the ceramide level in the cells exposed to chemotherapy agents is increased and leads to the inflammation response and ultimately the cell death. Typically, the ceramide targets are a variety of biomolecules and enzymes such as ceramide-activated protein kinase (CAPK), ceramide-activated protein phosphatase (CAPP), protein kinase C, and phospholipase D. Moreover, phosphoproteins in cells can be affected by ceramides altering many biological functions of the cell.[74,75]

2.3 Neural membrane lipids alterations in neurological disorders

After white adipose tissue, the brain is the organ most enriched with lipids in the body.[76] Therefore, it is obvious that any lipid alternation can heavily influence brain structure and function and it has been well established that many neurological diseases such as Alzheimer's disease (AD), Parkinson's disease (PD), multiple sclerosis, schizophrenia, ischemic stroke, anxiety, depression, and epilepsies are associated with lipid perturbations in the brain. To date, the actual cause and cascade of events in the progression of these diseases are not fully known due to the extensive complexity of the brain. Recently, the study of possible lipid alternation during these neurodegenerative disorders has been strongly focused in the hope of finding underlying pathogenic mechanisms and also treatments.[56,77] An overview of some of these disorders, their symptoms and the lipid systems involved are discussed here.

Alzheimer's disease as the most common form of dementia is a progressive brain disorder affecting the regions controlling memory and cognitive functions in the brain. In this worldwide neurodegenerative disease, a person's memory, ability to learn, reason, communicate, and daily activities are progressively impaired. According to previous studies, one of the molecular mechanisms suggested for this disease is lipid peroxidation by which the levels of lipids such as polyunsaturated fatty acids, PE, and PI are notably reduced in different regions of AD brains. Accordingly, changes in the composition of membrane lipid lead to a dangerous reduction of signal transduction and synaptic function and also to a series of serious neural membrane defects in AD brain regions.[78,79]

Parkinson's disease (PD) is another disorder, which is signified by selective degeneration of dopaminergic neurons, tremor, and rigidity. The etiology of PD remains unclear yet, lipid

peroxidation and oxidative stress caused by free radicals have been proposed to play a key role in the pathogenesis of PD. Recent studies in this regard demonstrated a role for oxidative stress in PD by marked increases in 8-hydroxy-2'-deoxyguanosine, a hydroxyl radical-damaged guanine nucleotide typically used to evaluate oxidative damage to DNA. A variety of markers of lipid peroxidation appeared to be notably raised in PD brain.[80,81]

Multiple Sclerosis (MS) is an autoimmune inflammatory attack against the myelin insulation sheath of nerve cells in the brain and the spinal cord harmfully disturbing the central nervous system and the communication between the brain and the body. Yet the reason for this neurodegeneration is not completely understood, but lipid peroxidation has evidently been believed to occur in MS.[82]

Schizophrenia is a genetic and chronic mental disorder affecting a person's thinking, emotional reactions, social behaviour along with hallucinations and delusions. The mechanism of this mental illness remains one of the most puzzling, although recent studies on the neurological deficits of schizophrenia have shown that alterations in membrane lipids may be involved in schizophrenia pathophysiology. Accordingly, abnormal changes in concentration and distribution of PC, ceramides, and fatty acids have been observed in the schizophrenic brain. Also, the levels of PC and PE in cell membrane are diminished in the brain during schizophrenia. These abnormalities occurring in lipid composition of the cellular membrane possibly change the structure and function of the cell membrane and thus the function of membrane-bound proteins, availability of cell signaling molecules, and the behaviour of neurotransmitter systems. This can offer new insight into the role of lipid profiles in schizophrenia pathophysiology.[82-84]

Ischemic stroke occurs as a result of an obstruction of a blood vessel supplying blood to the brain by a blood clot, which then leads to the loss of neurological function and brain injury. This is marked by failure in lipid functions giving rise to lipid alteration and ultimately cell death. Recent studies have revealed that a variety of lipid disturbances appear to occur in rat brain exposed to ischemic stroke. In the ischemic brain region, the potassium ion adduct of PC exists at a lower concentration; whereas the sodium ion adduct of PC is present at higher concentration. Considerably higher levels of glysoglycerophospholipids, sphingomyelin, and DAGs are accumulated in the injured brain showing that the metabolic pathways of lipids are altered in the inflammatory cellular response.[85,86]

3. Biological Mass Spectrometry Imaging

For decades, the study of biological samples in particular tissues and cells have offered many challenges to the biologist due to their complex chemical and structural properties. So far, microscopic techniques and fluorescent labeling have been well known as the most powerful tools to image the distribution of biological molecules and to investigate the physiological processes happening within a biological system. However, these techniques basically suffer from a limitation that they do not provide direct chemical information, and they require an antibody label, probe, or stain to function. These labels might lead to a change in the chemical and physical properties of the labeled molecule thereby changing its intracellular distribution. Finally, to visualize the molecules of interest in biological systems, probes and antibodies might not always available or be too unspecific to give accurate results.

In the past few decades, mass spectrometry imaging (MSI) has evolved as a powerful label-free (although isotopic labels are sometimes used) technique for identifying, imaging and visualizing the intensity distribution of endogenous biological molecules such as peptides and lipids in the biological samples. The MSI technique provides many advantages compared to microscopy such as extremely low detection limits, parallel detection of multiple analytes in complex biological samples, and the ability to provide spatial as well as chemical information at once.[87-89]

3.1 Mass spectrometry: brief introduction and history

Mass spectrometry (MS) is a powerful analytical method used to elucidate the structural and chemical composition of different molecules in a sample based on measuring the mass to charge ratio (m/z) of charged particles. It is used to identify the composition of various chemical compounds. In general, MS instruments consist of three major components; ion source, mass analyzer, and detector. First, molecules of the sample are introduced into the gas phase and are ionized in the ion source. The ions produced are then subjected to the mass analyzer where they are separated and sorted based on their m/z ratio. The separated ions reach the detector and a signal is then sent to a data system which creates a mass spectrum.[90,91]

J. J. Thomson, a physicist who described the electron in 1897, developed the first crude ‘mass spectrograph’ by which he measured the atomic weights of elements. In this device, ions

created in discharge tubes were introduced into electric and magnetic fields where they travel through parabolic trajectories. Subsequently, the produced particle rays were detected on a fluorescent screen or photographic plate. A later version of his instrument was completed by Thomson's students who built a real mass spectrometer. In this device, ions could be distributed by mass and then focused by velocity.[92]

In the 1940s Professor Alfred O. C. Nier designed and built some devices providing more sensitive and precise measurements of isotopes and their ratios. This was a revelation in mass spectrometry making this technique attractive for public attention. He designed a 60° sector field instrument, the so-called Nier-Johnson mass spectrometer, in which electrostatic and magnetic analyzers were combined in an exclusive combination. By further industrial development, the double-focusing magnetic sector instruments were introduced in which an electric sector was employed to correct kinetic energy spread of ions before separation in the magnetic field, in spite of the fact that this generation of mass spectrometers led to better mass accuracy, peak capacity, and resolution, those instruments were very expensive. This drawback led to developing some cheaper alternatives such as time-of-flight (ToF), quadrupole, and ion trap mass spectrometers.[93]

3.2 Time-of-flight mass analyzer

The time-of-flight (ToF) mass analyzer, introduced by William E. Stephens in 1946, led to a significant increase in the MS sensitivity due to a very high transmission and wide mass range.[94] The unique advantages of a ToF analyzer include detection of all the ions generated, high mass resolution, parallel detection and direct examination of multiple ionic species from the sample making this analyzer ideal for the analysis of complex biological samples.[95] In the ToF analyzer, ions are accelerated with a high voltage into a field-free zone where they are separated by differences in their velocities. With the same kinetic energy, the velocity of an ion in the flight tube is directly proportional to its mass and inversely proportional to its charge. This relationship is described in Equation 3.1 where kinetic energy (E Kinetic) is a function of mass (m) and velocity (v), as well as a function of particle charge (q=Ze) and potential (V).[95,96]

$$E\ kinetic = qVs = ZeVs = \frac{1}{2}mv^2 = \frac{1}{2}\left(m\frac{l^2}{t^2}\right) \quad \text{Equation 3.1}$$

Time of flight for a specific ion can be calculated by Equation 3.2, given the length of the flight tube (l).

$$t = l\frac{1}{\sqrt{2E}}\sqrt{m/z} \qquad \text{Equation 3.2}$$

The lighter ions move faster in the flight tube and reach the detector sooner than heavier ions. Despite the fact that ions with the same mass to charge ratio should have the same flight time, the initial temporal, energetic, and spatial distributions among generated ions species can result in poor mass resolution even for ions with the same m/z ratio. As linear ToF mass analyzers were not capable of resolving these issues properly, their mass resolution is considerably reduced. However, several technological advances have been developed over the years, such as delayed extraction techniques and dual stage reflectrons to improve the resolving power of ToF mass analyzers. In the delayed extraction technique, there is a time-specific delay applied on the ions generated before they are extracted into the mass analyzer using high voltage pulses. This leads to a decrease of the variation in kinetic energy between ions with very similar m/z ratio. In the reflectron (Figure 3.1), the ions are decelerated and reflected back into the drift tube by a series of electrostatic rings at the end of the flight tube. The reflectron increases the length and distance of the flight path and also remedies the energy spread among ions with similar m/z ratios. High energy ions penetrate longer into the reflectron than lower energy ions with the same m/z ratio, thus the ions with similar m/z but different kinetic energy reach the detector at the same time leading to improvement of the mass resolution.[97-99]

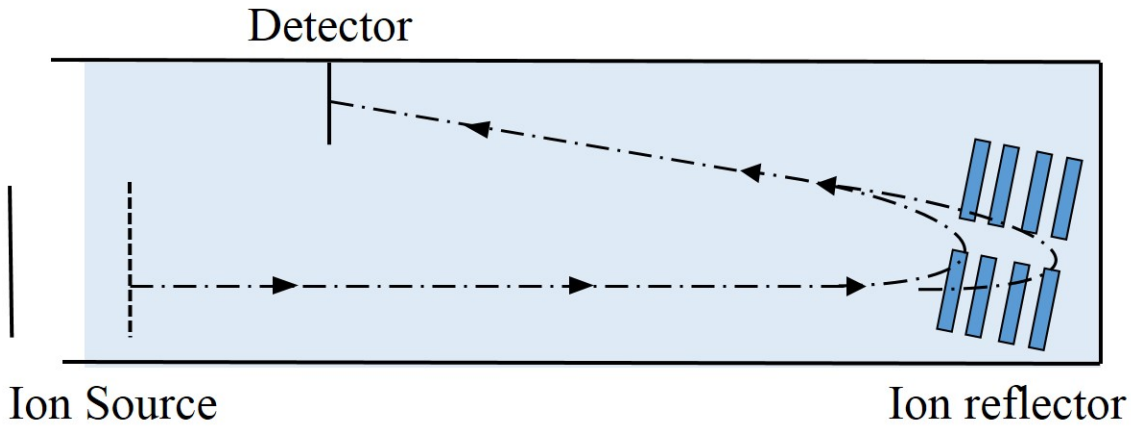

Figure 3.1 Schematic illustration of Time of Flight (ToF) analyzer with ion reflectors.

3.3 Mass spectrometry imaging

Mass spectrometry imaging (MSI), a rapidly growing subfield of chemical imaging is capable of combining the molecular mass analysis and spatial information to provide visualization and localization maps for a variety of atoms and molecules on complex surfaces. Generally, in MSI techniques, ion images are produced by rastering across the surface of the sample to collect a series of mass spectra from an ordered array of spots. After the data acquisitions, ion images for the analytes of interest is mapped and visualized by a color scale which represents the intensity distribution for individual chemical species along the sample surface (Figure 3.2). In recent years more interest in MSI, particularly for biological studies, has rapidly and continuously grown leading to the development and application of secondary ion mass spectrometry (SIMS) and matrix-assisted laser desorption ionization (MALDI). SIMS allows detection of small molecules (<1000 Da) at a higher spatial resolution over a lower mass range, whereas MALDI with the ability to ionize larger molecules is well suited for detection of much broader mass range (~500 Da to >100 kDa), albeit at lower spatial resolution. These imaging techniques will be discussed in more details later in this thesis.[87]

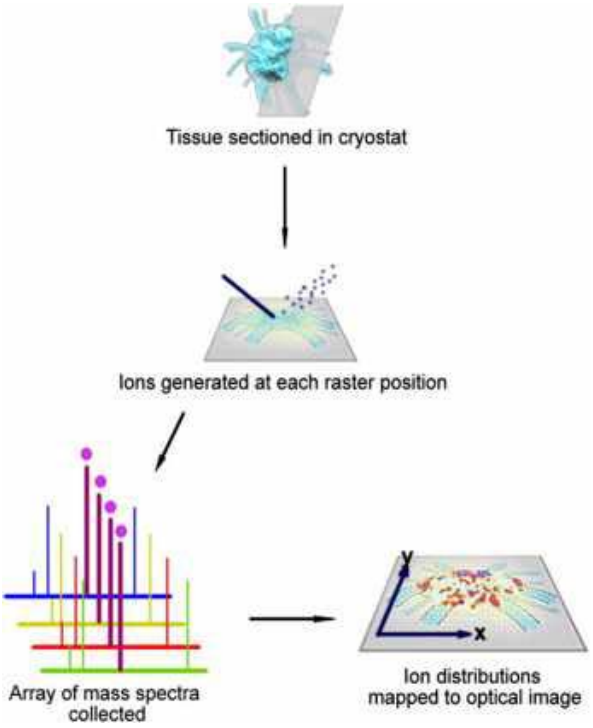

Figure 3.2 Representation of creating the ion images in MSI. The sample is analyzed in a raster array in the mass spectrometer and consequently, by collecting mass spectra for each spot and processing this array, an ion density map of a chosen m/z can be obtained across the sample in a two dimensions image. Image reproduced with permission from Greer et al.[100]

3.4 Advantages of MSI

MSI is a promising technique for sample surface analysis. Complimentary to other imaging approaches, MSI advantageously allows label-free or isotopically labeled species detection, high chemical specificity, high accuracy, and broad analyte coverage. The ability of MSI techniques in combination of the chemical specificity and spatial analysis of surfaces allows the analyst to obtain spatial localization of several different compounds, complex biomolecules and parallel detection of multiple analytes. MSI offers high sensitivity to image molecules present at very low abundance inside systems as small as cells. Current instruments are able to detect molecules in concentrations of approximately 500 attomol allowing components from a single cell to be detected.[101]

MSI methods provide high spatial resolution biomolecular analysis. Depending on the ionization technique used, the spatial resolution obtained varies. For instance, MALDI can be focused to the size of 10 μm in diameter,[102,103] whereas ToF-SIMS routinely provides submicron spatial resolution.[104,105] The new generation of mass spectrometers is capable of separating and thus detecting ions with very high mass resolution. High mass resolving power is typically used to provide spatial features which routinely are not able to be revealed with low-resolution techniques.[106] The time required for analysis and imaging of sample is also considered as a crucial aspect of any imaging technique. For MSI, the image acquisition time is determined by the sample area, the desired spatial resolution, and also the repetition rate of the probe beam and generally takes minutes to quite a few hours. Due to these unique characteristics, MSI is well known as a powerful analytical tool in biological studies to measure the distribution of many classes of compounds ranging from atoms to larger intact molecules such as peptides and proteins.[87,100,107]

3.5 Biological sample preparation for MSI

The quality of the sample directly influences the sensitivity, reproducibility, and accuracy of the imaging experiment in MSI. Therefore sample handling and preparation is an important concern for any biological imaging study. A good sample preparation for MSI experiments needs a practical and productive procedure for routine analysis. Additionally, several important properties of samples including minimal sample contamination, sample integrity under ion bombardment, morphological preservation, and minimal redistribution of diffusible species have to be achieved in an appropriate sample preparation. Among these requirements, in particular, preserving the chemical and spatial integrity of biological samples can be

challenging for MSI since it has to be performed under biologically unfavourable vacuum conditions. A variety of protocols have been established for both tissue and cellular samples, the most commonly used procedures are reviewed here as below.[87,108]

3.5.1 Tissue preparation

MSI protocols for tissues commonly require steps in which the tissue samples are fixed, sectioned, mounted, and/or dried. Cellular samples are also fixed and then analyzed in a frozen hydrated state,[108,109] which will be discussed in more detail later in the cell preparation section.

To minimize sample degradation or delocalization and also to keep the sample stable under high vacuum, fixation needs to be applied on tissue samples immediately after dissection and also on cellular samples after removal from culture media. Traditional chemical based fixation procedures, which influence the location of ions and molecules, thereby change the natural cell chemistry and should be avoided especially for lipid-based analysis.[110-112] In contrast, cryofixation methods which involve plunge freezing, high-pressure freezing, and possibly subsequent freeze-drying are able to preserve the integrity of the tissue samples gaining great interest for IMS techniques. In plunge-freezing, the tissue sample is submerged in liquid propane at -185°C and subsequently transferred and stored in liquid nitrogen or in a -80 °C freezer. In high-pressure freezing, the sample is pressurized to 2000 bar in a small container and at the same time the outer surface of the container is cooled with a jet of liquid nitrogen. The freezing process in both methods is so fast that amorphous ice is formed from the water content on the surface of the specimen. This is advantageous since the formation of ice crystals leading to molecular and morphological displacement is considerably remedied in plunge-frozen samples thereby structural damage of the sample can be prevented.[110,113]

After freeze-fixation, tissue samples are brought to -20º C and sliced into 5-15 μm thick using a cryomicrotome. The tissue section is then thaw-mounted on a conductively coated glass or metal sample plate. Prior to MSI analysis, tissue sections are freeze-dried in which the water content of the sample is gradually sublimated and then brought to room temperature and dehydrated under vacuum conditions (mbar). Freeze-drying is an acceptable procedure for the preparation of tissue samples where fine spatial resolution is not needed.[112,114]

In addition to cryomicrotoming, there are other protocols widely used for surface preparation of tissue samples including freeze fracture, frozen hydrated analysis, etching by temperature, or etching with a defocused etching gun such as C_{60}^{+} or low energy Ar gas cluster ion beam

(GCIB). These are also used for cellular samples[109,115] and are discussed in cell preparation section.

3.5.2 Cell sample preparation

Different methods of plunge-freezing combined with freeze-fracturing and frozen hydration are widely used for cultured cells.[116-118] In particular, frozen hydrated sample protocols for the MSI analysis of cells, first described by Chandra and coworkers, have become the gold standard for cell-based studies.[119,120]

In this technique, cells are cryo-fixed via the freeze plunging method, which was described above. Samples are then analyzed without drying while they are kept frozen by a liquid nitrogen cooled stage throughout the analysis. Cell morphology and spatial integrity of diffusible molecules are preserved with this method. Moreover, a significant enhancement of the molecular ion signal, especially for phospholipids, has been revealed using the frozen-hydrated sample preparation procedure due to the reduction of damage accumulation in liquid nitrogen temperatures. Also, the condensed water matrix covering the surface of the sample can act as a proton source to protonate and to enhance the signals of protonated ion species. In the freeze-fracture procedure, the samples are plunge frozen while being sandwiched onto two silicon shards which are opened in the instrument under vacuum.[121] Subsequently, the fractured and fresh surface of the sample is exposed to analysis. The protocol eliminates human and external influences protecting the sample from possible environmental contamination. Furthermore, the method can also be used in subcellular studies fracturing of the inner sections of the cells is possible, although achieving a consistent, reliable and reproducible fracture plane is an issue here and this hinders the analysis. Accordingly, some alternative strategies including etching by use of a slightly elevated temperature or sputtering with cluster ion guns can be used to overcome the topographic problems observed with freeze fracture. In etching by temperature, the temperature is gradually increased to a critical point so that the top layer of condensed water is slowly sublimed revealing the biological sample below. When sputtering with a C_{60}^{+} gun or Ar GCIB is used, the water overlay from the sample is removed without damaging the subsurface. These two methods help flatten the sample surface and thereby remedy the topographic problems. With these methods, it is also possible to preserve sample morphology and keep the sample from environmental contamination, although the sample handling is complicated and time-consuming for these procedures.[109,115]

3.6 Pitfalls of MSI

Compatibility of the samples with room temperature as well as high vacuum that is usually used with MSI experiments is important. Unfortunately, some molecules are very sensitive and easily degraded at room temperature in a couple of minutes. In essence, there is the possibility of molecular diffusion in all types of sample treatments at room temperature, which negatively influences spatial resolution, data reproducibility, and the quality of the images. The sample preparation process should therefore be very fast, and not expose the samples to the air, moisture, or high temperature. There are various compounds present in biological tissue sections such as matrix ions, lipids, proteins, oligonucleotides, carbohydrates, and salts which can unfavorably impress efficiency of desorption and ionization and also inhibit the optimal detection. This phenomenon, called ion suppression, in which the ionization process is less efficient causes reduction the quality of the MSI analysis.[87,122]

3.6.1 Resolution and Sensitivity

In general, there is a trade-off between lateral resolution and the number of ions generated. This is considered to be the main analytical issue for analysis limitations in instrumental work at the cellular level. At high lateral resolution, there is a significant decrease in the number of available analytes to be ionized and detected. In other words, lateral resolution is increased at the cost of sensitivity. However, there have been some surface treatment methods developed to improve sensitivity which [109] will be discussed in more details later in this thesis.

In this thesis, I mainly focused on the use of two common techniques of MSI including MALDI and SIMS in biological samples studies. In the following two chapters, I will discuss these innovative analytical techniques, strengths, weaknesses, and current efforts to address the main challenges in this area.

4. Matrix Assisted Laser Desorption Ionization (MALDI)

MALDI is a soft ionization laser-based method applied in mass spectrometry. It has been known as one of the most powerful methods for analysis and detection of a wide range of biomolecules from several hundred to several tens of thousands of Daltons, which covers a variety of biomolecules including intact lipids, peptides, proteins, and polymers.[87]

4.1 Principles of MALDI

The combination of a matrix and laser desorption is the main characteristic of MALD. As illustrated in Figure 4.1, sample to be analysed is first coated with a thin homogeneous layer of a matrix, typically a low molecular weight organic acid. In this step, the matrix application on the sample surface plays a key role for the soft ionization of the analyzed biomolecules. In fact, a large amount of the proper crystallized matrix molecules is mixed with the analyte at a molar matrix to analyte ratio of 10^3-10^5:1. By vaporization of solvent, the biomolecules from the sample surface are co-crystallized with matrix and extracted which forms analyte-doped matrix crystals.[87,123]

The matrix crystals containing analyte are irradiated with a pulsed laser and the matrix molecules absorb the majority of the laser energy. The absorbed energy of the laser with the matrix/analyte mixture causes desorption of the analyte molecules into the gas phase. Moreover, in the gas phase the organic matrix molecules aid the ionization of analytes via some chemical and physical ionization mechanisms. These mechanisms include excited state proton transfer, gas-phase photoionization, and ion-molecule reactions. Among the known mechanisms, ion formation through proton transfer in the solid phase before desorption or in the gas-phase is the most recognized. Here, matrix serves as a proton donor or acceptor ionizing the gas analyte molecules to form molecular ions commonly in the singly charged state. Proton transfer between the matrix and the analyte yields protonated ($[M+H]^+$) or deprotonated ($[M-H]^-$) ions from neutral analyte molecules [M]. The resulting ions by protonation are detectable in positive ion mode and the deprotonated species can be identified in negative ion mode. Analytes can also form adducts with salts ($[M+Na]^+$) through cation transfer. Furthermore, some multiply charged ions and a lot of fragments can be usually detected, although as MALDI is a soft ionization technique, still little fragmentation of

molecules occurs during ion formation. Typically as the analyte must be incorporated into the matrix crystals causing a complete separation of analyte from contaminants in the solid phase, this makes MALDI less sensitive to contaminants such as salts, buffers and detergents compared to other ionization techniques. A high concentration of contaminants such as buffers can, however, have a negative effect on the desorption and ionization steps. In order to eliminate this effect from contaminants, prior purification is typically carried out.[87,91,124]

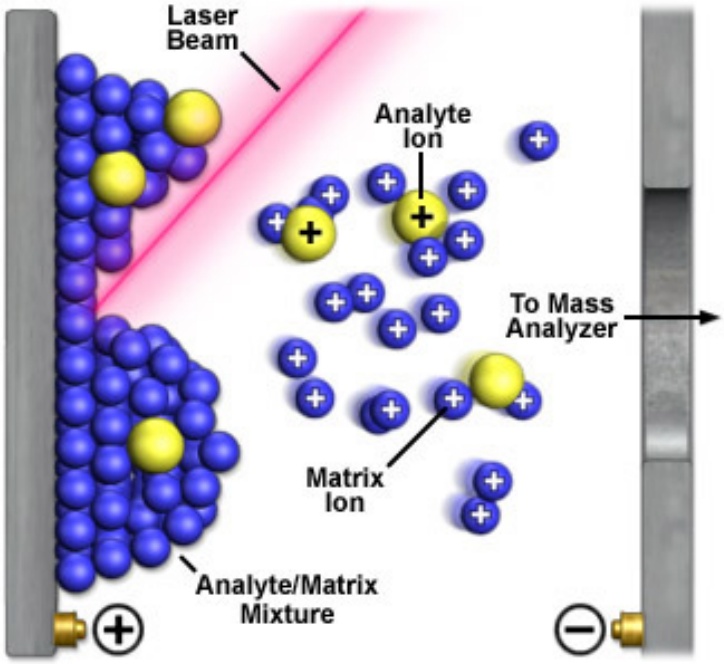

Figure 4.1 Principle of MALDI ionization: the formation of ions during MALDI. Image reproduced with permission from Chughtai et al.[87]

4.2 Spatial resolution in MALDI imaging

Spatial resolution is governed by the distance between two pixels, and generally defines the quality of images. The commercial MALDI instruments that are currently available can provide a typical spatial resolution about 10 μm, which is the minimum achievable laser beam size in MALDI. In fact a high spatial resolution (<10 μm), which is indeed desirable for biological imaging down to cellular level, is not practically attainable.[125] Therefore, the spatial resolution can be one of the major challenges in MALDI imaging for biological applications. In essence, the spatial resolution in MALDI is practically determined by the spot size of laser and the matrix crystal size. Modification of any of these two parameters can help to improve

the spatial resolution. Strategies have been introduced to decrease the spot size of the laser in imaging applications. One of them is called the oversampling approach in which the laser entirely ablates the sample at positions smaller than the laser step size leading to the acquisition of signals from adjacent spots spaced in an area smaller than the spot size of the laser and enhancing spatial resolution.[126] Some instrumental approaches have been also developed using lenses or other optic devices to achieve high spatial resolution imaging in MALDI. For instance, Caprioli and co-workers developed a specific geometry to irradiate the laser from the back side of the sample, which was located on a transparent substrate. They were able to successfully focus the diameter to less than 1-2 μm for laser beam size.[127]

4.3 Overview of sample preparation for MALDI

As discussed in chapter 3 of this thesis (Biological Mass Spectrometry Imaging), the quality of the sample has a direct impact on the sensitivity, reproducibility, and accuracy of MS imaging. Also in MALDI imaging, sample handling is again critical requirement for ensuring that integrity and spatial organization of the analytes on the sample are preserved with the minimum delocalization and degradation. All of the treatment procedures from the sample collection to analysis need to be adequately fast to avoid rapid tissue degradation. To choose an experimental strategy, the nature of the sample and the biomolecules of interest are major considerations. The sample preparation protocol, particularly in case of tissue sections, consists of different steps including sample collection, sectioning into thin slices, mounting on conductive indium tin oxide (ITO) coated glass slides, freeze-drying, washing of the tissue and application of matrix. Among the above steps, two phases of the washing and matrix deposition will be debated here.[124,128]

4.3.1 Sample washing

Washing is required to remove native salts and other undesirable molecules from the surface of the tissue so that they do not influence the measurement. In fact, salts, which are easily diffusible molecules, practically suppress ionization through direct ionization or adduct formation with the proteins and peptides. This obscures the signals of the analyte to be detected. In addition, the salt content of the sample surface can negatively affect the matrix crystallization process. Washing is carried out either by immersion of the slide carrying the

tissue in washing solution or application of the solution is applied on top of the tissue by use of a pipet. Based on the analyte of interest, there are several washing procedures and solutions. The standard washing protocol generally uses a brief 70% ethanol wash to remove salts and is followed by temporary fixation with 90% ethanol. In lipid analysis, a low concentration (5-10 mM) of a volatile and MS friendly salt solution such as ammonium formate is usually recommended for washing high salt containing samples to partially remove the salt content. For analysis of high mass compounds, for instance peptides and proteins, washing with an organic solvent such as chloroform or xylene is applied to remove high lipid content. However, washing procedures using organic solvents can cause delocalization of the biomolecules of interest. [87,124,129]

4.3.2 MALDI matrix choice and application

Matrix deposition on the sample surface is usually the last step of sample treatment and plays a crucial role in MALDI imaging. Analyte detection is critically affected not only by the choice of a proper matrix and solution composition but also by the matrix deposition method which is needed to preserve spatial distribution of analytes across the sample leading to high-quality spectra and ion images. In this regard, it is necessary to select a proper matrix compound and also matrix application method in MALDI analysis. A suitable matrix molecule needs to have several practical features including the stability of matrix in vacuum conditions, the ability in absorbance at laser wavelength, solubility of both matrix and analyte in solvents used in matrix solution. Additionally, the chemical properties and mass range of the matrix molecule has to be considered in order to minimize interfering between analyte and applied matrix. Many different kinds of matrix and solvent combinations have found applications in MALDI for the detection of different classes of molecules in the mass range from several hundred Da to several hundred kDa. There are several kinds of matrices that are derivatives of benzoic acid, cinamic acid, and picolinic acid with different properties commonly used in MALDI analysis. Alpha-cyano-4-hydroxycinnamic acid (CHCA), which has good solubility in organic solvents, is commonly used for lower molecular weight peptides, small proteins, and glycopeptides. CHCA has the ability to produce small homogenous crystals, which leads to obtaining a good spatial resolution especially in the imaging analysis of peptides. Additionally, it is possible to wash samples on the target with water as part of the preparation since this matrix is not soluble in water. A large amount of

fragmentation occurs with CHCA and is its main disadvantage. Another organic matrix commonly used in MALDI analysis is 2,5-dihydroxybenzoic acid (DHB), which is simply soluble in both water and organic solvents. DHB is suitable for phospholipid detection and has an advantage that it is less sensitive to contaminants such as salts and detergents than other common matrices. The DHB matrix typically forms large crystals after drying on the surface of samples. These large crystals can alter the homogeneity of the sample surface from spot to spot leading to a significant decrease in the spatial resolution, which is the main disadvantage for this matrix compound. Sinapinic acid (3,5-dimethoxy-4-hydroxycinnamic acid, SA) is a common organic matrix for higher M_W proteins. In contrast to CHCA and DHB, which have been commonly used for detection of lipids in positive ion mode, 9-aminoacridine is properly used as a suitable matrix for detection of lipids and metabolites in the negative ion mode of MALDI.[87,128,130]

A matrix solution typically consists of an organic solution such as ethanol, methanol or acetonitrile, an organic matrix substance, and trifluoroacetic acid (TFA). In the matrix solution, the solvent extracts the analyte from the sample and the matrix crystallization occurs after rapid evaporation of the organic solvent. TFA is a proton donor and increases the number of available protons for ionization thereby assisting the protonation of the analyte molecules. The ratio of matrix to the organic solvent combination, the concentration of matrix, and the concentration of TFA are key factors influencing the incorporation of the matrix with the analytes of interest and also the crystallization process. The percentage of the organic solvent is generally prepared depending on the hydrophobicity of the analyte molecules of interest and for tissue analysis the ratio of 50:50 of acetonitrile/water or ethanol/water is commonly used. A typical concentration of TFA for most MALDI analyses is 0.1 %.[87]

Deposition of the matrix on the sample surface, which must be performed before MALDI analysis, is a crucial step in sample preparation. The reproducibility of matrix deposition on the sample surface and the homogeneity of the deposited layer of organic matrix are important factors in order to obtain similar and uniform desorption of analytes along the sample surface. In MALDI imaging it is significant that the organic matrix deposited on the sample surface forms crystals with a size equal to or smaller than the size of the laser spot size in order to obtain high spatial resolution ion images. On the other hand, if the crystal size of the organic matrix for detection of intact biomolecules is too small it will deliver low sensitivity for MSI detection. Thus, the size of crystals has an important role in determining the sensitivity in MSI

detection. Desorption and ionization techniques, required sensitivity, and spatial resolution, are parameters defining the proper crystal size of the dried organic matrix when performing MALDI analysis. Another fundamental factor in MALDI imaging analysis is the thickness of the organic matrix layer deposited in which insufficient matrix on the sample surface gives rise to unstable analyte signals.[89,128]

In recent years, different methods have been developed to deposit the organic matrix on the surface of tissue sections. These methods, which can be dry or wet, are used based on a required spatial resolution for imaging and the abundance of the analytes in the sample. Deposition of the matrix can also be performed either manually or automatically. Manual procedures suffer from poor reproducibility, whereas automated devices provide better reproducibility and control during the extraction process leading to the possibility of comparison between different samples. In both cases, a particular issue is the formation of possible homogenous crystals that can trap most of the analytes without significant diffusion of molecules.[87,131,132] The most commonly used method is spotting, where sample surface is covered by nano or micro-droplets of matrix solution. Another method employs a sprayer by which smaller droplets of matrix solution are sprayed resulting in a thin coating of matrix on the surface and better spatial resolution compared to spotting. However, if the sample gets too wet during spraying, chemical delocalization of biomolecules might occur across the sample lessening the reproducibility of this method. Spotting and spraying can be done manually using a micropipette and an airbrush, respectively. Most recently, automated devices including inkjet printers and acoustic dispensers developed to use for spotting, and also automatic pneumatic sprayers (pneumatic sprayer, airbrush, the TM sprayer system from HTX) and vibrational sprayers (ImagePrep Device from Bruker Daltonics) for spraying have become commercially available.[133-135]

In addition to wet matrix deposition methods, a non-commercial and a solvent-free method called sublimation has been developed in which the matrix is sublimed and deposited on the sample surface in a vacuum. A homogenous coverage of the sample surface by the organic matrix with very small crystals that is appropriate for high spatial resolution MALDI imaging can be obtained by the sublimation method. Deposition of the organic matrix by sublimation method provides a high purity matrix directly deposited on the sample and also as a solvent-free technique it prevents analyte delocalization on tissue surface, which is a notable issue for MALDI imaging. As an advantage the system designed for deposition of organic matrix by sublimation is relatively straightforward and inexpensive.[87,128]

However, sublimation as a solvent-free matrix deposition suffers from the poor extraction of the analytes compared to wet methods. In order to compensate for this disadvantage, re-wetting of the sample surface using TFA or an organic solvent can be helpful enhancing the miscibility of matrix and analyte molecules at the surface of the sample.[103]

4.3.3 Nanoparticle application; an alternative to the organic matrix

Nanoparticles (NPs) made from a number of substances can be applied as an alternative surface modification to the standard organic matrices.[136] This surface modification is well known as a new technical approach called surface assisted laser desorption ionization (SALDI). The use of NPs in the range from 2 to 100 nm from several materials reveals their ability to absorb the laser energy and then transfer it into heat allowing ejection and ionization of molecular species. The use of NPs offers some advantages to common organic matrix deposition. First, due to the lack of formation of matrix crystals using NP deposition, a higher spatial resolution can be achieved if a smaller laser beam diameter is applied. Compared to the common organic matrices deposition, the use of NP sample modification offers a better selectivity and sufficient sensitivity for biomolecules.[137]

Among several NP materials, gold nanoparticles (Au NPs) have been extensively used in SALDI to analyze glycosphingolipids, triacylglycerides, and carbohydrates.[138-141] In analysis using NP surface modification; ejection and ionization of molecular species appear to be achieved by a heating process. The interaction of laser irradiation excites electrons in the Au NPs producing heat, that is transferred to the analytes, leading to desorption and ionization process.[142,143]

In comparison with MALDI, the use of NPs is a potentially beneficial matrix material for laser desorption ionization (LDI) since they enable submicron spatial imaging and also offer complementary chemical information to the organic matrices commonly used on biological studies. This approach was used as part of the work presented in paper II.

5. Secondary Ion Mass Spectrometry (SIMS)

SIMS is an ultra-surface sensitive, ultra-high vacuum (UHV) analytical technique in which a solid sample is bombarded by a focused and often pulsed energetic particle beam, a so-called primary ion beam. Impact of primary ions leads to ejection of secondary species (positive, negative, and neutral) from the surface of the target. The charged particles are collected, separated, and analyzed in a mass analyzer (Figure 5.1). The secondary ions are representative of the species present on the surface, and so SIMS allows one to obtain the chemical composition of a surface.[144]

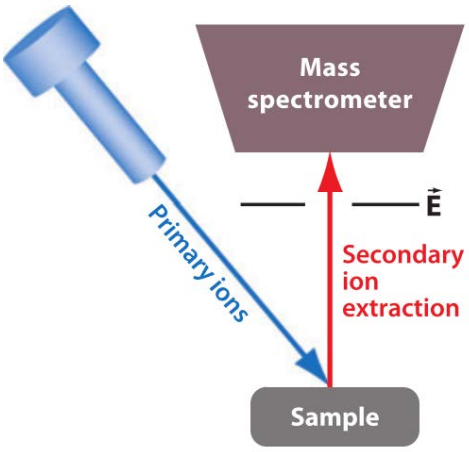

Figure 5.1 A simple illustration of a SIMS instrument. A solid sample is bombarded by a focused primary ion beam leading to emitting a fraction of the charged particles called secondary ions from the surface of the target. In mass spectrometry extraction, collecting, and analyzing of the secondary ions provides information about chemicals and composition of the analyzed surface. Image reproduced with permission from Boxer et al. [145]

5.1 Basic principles

Species ejection in SIMS occurs when a primary ion beam with an appropriately high energy, about 5-40 keV, impacts the sample surface and causes a cascade of collisions in the target rising to the surface by transferring kinetic energy in the lattice of sample atoms or molecules (Figure 5.2). As some of these collisions return back to the surface and if an atom or groups of atoms receive enough energy in a suitable direction enabling them to overcome the surface binding forces then species can be ejected from the surface. The majority of these ejected molecules are neutral and only around 1% of them are ionized as they leave the surface.[87,109]

SIMS is widely used in two modes, static and dynamic. Basically, static SIMS is performed using a low energy pulse of the primary ion beam to extremely sputter the surface with low ion doses. In static SIMS, the sample surface is not significantly damaged and less than 1% of the top monolayer is impacted by primary ions providing atomic or molecular information. In the dynamic SIMS mode, a much more energetic primary ion flux is used to probe the sample, which leads to interrogation of the sample surface with significant alteration by the primary ion beam. This mode of SIMS is best known for bulk analysis of elements, small fragments of molecules and depth profiling.[145,146] These two operational modes of SIMS will be discussed more in section 5.4 in this thesis.

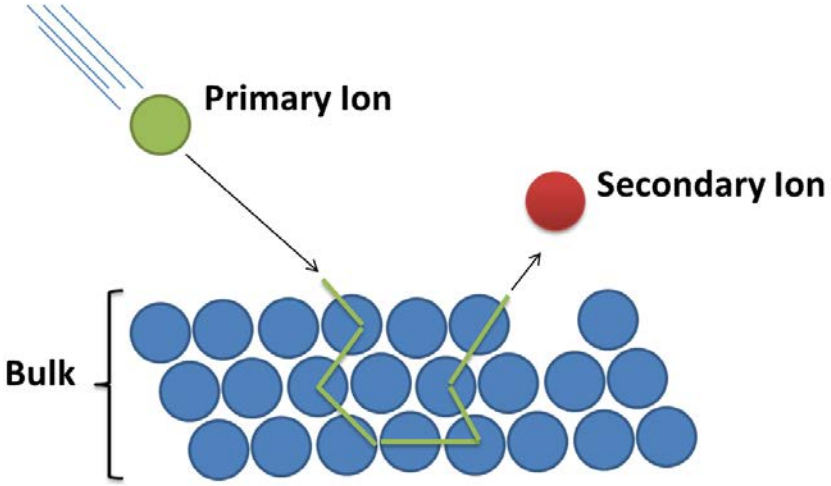

Figure 5.2 Schematic representation of sputtering through a collision event generated from the impact of the primary ion (green) upon the sample (blue) thereby transferring energy to the sample, which is then distributed through different atoms (green lines) and leads to ejection of secondary ion (red) from sample surface.

5.2 Generation of secondary ions

There are two processes can be considered for secondary ion formation during SIMS analysis. First is sputtering in which atoms and multi-atomic clusters are desorbed from the surface, and the second is that sputtered species are ionized gaining or losing electrons.

5.2.1 Sputtering

Sigmund's linear cascade theory introduced in 1981 has been the most accurate model to describe the sputtering process caused by a monoatomic primary ion beam impinging on a

surface.[147] Sigmund assumes the atoms of the solids to be hard spheres that follow Newtonian mechanics that can be sputtered using a beam at low current and fluence. Based on this theory, the sputtering process using high-energy beams implicates a knock-on effect and electronic sputtering effect. For the low energy beam (few keV), the theory was developed to involve elastic collisions. In this process, as the primary ions strike over a sample surface, they penetrate into the sample and transfer its energy to the atoms/molecules of the surface. The ejection of atoms and molecules happens when sufficient impact energy is provided to overcome the surface binding energy. This theory has been successfully used to describe a monatomic primary ion impacting a single component sample with yields depending on the mass and the energy of primary ions. It is important to note that this model might not be suitable for multi-component systems since the transfer of energy is directional and not isotropic. In this case, another model might be needed to describe these complex systems.

5.2.2 Ionization

Based on the nature of the sample and the technique used which has an effect on the ionization of the sputtered species, only a small fraction of particles which are ejected from sample surface is ionized in the SIMS process. The ion yield is highly dependent on the electronic properties of the environment of the analyte in the sample, known as the matrix effect. In general, metalic samples become ionized by swift electronic transitions while in organics, ionization occurs by losing or gaining a charged species, typically a proton, to form $[M+H]^+$ or $[M-H]^-$ ions, but salt adducts of sodium, chlorine and potassium are also commonly detected. Various models have been developed to explain the ionization occurring during a SIMS process. One of them is the desorption-ionization model which was introduced by Cooks and Busch in1983.[148] This model regards desorption and ionization processes as two separate processes with different mechanisms. Ions are generated by desorption followed by two chemical reactions. The first is ion/molecule reactions or electron emitting reactions, which can occur at the top of the sample surface. The second involves dissociation of the parent ions, which can possibly generate fragment ions as well.

5.3 Basic equation for SIMS

As described above, the SIMS technique is based on the analysis of secondary ions with the yields depending on the electronic state of the surface. The relationships between the factors used to govern the secondary ion yield are represented in the SIMS equation [149] as shown in Equation 5.1

$$I_m = I_p \, Y_m \, \alpha^{\pm} \theta_m \, \eta \qquad \text{Equation 5.1}$$

Here, I_m is the secondary ion current, Ip is the primary ion current, Y_m is the sputter yield of secondary species including ions and neutral, $\alpha^{\pm}$ is the ionization probability of the species m to positive and negative ions, θ_m is the fractional concentration of species m in the surface layer, and η is the transmission fraction of the analysis system.

Two key parameters that govern sample extraction in SIMS are sputter yield and ionization probability. The sputter yield is the total particles, including neutrals and ions, which are desorbed from a surface per primary ion impact. The yield depends on topography and the nature of the sample and also the mass, charge, energy and primary ion current. The primary ion density is operator dependent but the transmission is commonly constant for each instrument.[150]

5.3.1 Matrix effects

Y_m and $\alpha^{\pm}$ are the two fundamental parameters that are highly dependent on the properties of the species in the sample and the surrounding environment (the matrix). Matrix effects can lead to different secondary ion yields for the same compounds with the same concentration when two different matrices are used despite all other parameters being equal. This is known as the matrix effect, which plays a key role in SIMS quantitative analysis. Matrix effects lead to enhancement or suppression of the ionization rate of an analyte in the presence of other species and the secondary ion yield is not directly proportional to its concentration in the sample rather but is influenced by the chemistry of the environment. Therefore, it is normally not possible to precisely quantify components on a sample surface and quantitative SIMS analysis is difficult. SIMS can be considered a “semi-quantitative” technique, by comparison, the signal intensity of one species in one sample to the intensity of the same species in another sample.[144,151]

5.3.2 Damage cross-section and secondary ion formation efficiency

Two other important parameters are the damage cross-section (σ), and the efficiency (E) of ionization. The damage cross section has been defined as "the average surface area depleted resulting from a single ion impact" by Kötter et al.[152] in 1998 and can be described as Equation 5.2:

$$\sigma = N_{des}/N_o \qquad \text{Equation 5.2}$$

where N_{des} is the average number of molecular species that disappear from the surface upon one single primary ion impact. N_o is total number of molecular species M in the unit area of 1 cm^2 of the topmost monolayer.

In essence, the damage cross-section refers to the area of the sample surface that is altered following a single primary ion collision; thereby the molecules of interest thought to be damaged. It depends on the nature of the primary ion beam, properties of the secondary particles, the structure and the composition of the sample surface.

In order to provide a relation between the secondary ion yields and damage cross-section, the efficiency was introduced. This provides a measure of the signal available that can be obtained from an area before the surface becomes damaged. It is defined as a ratio of secondary ion yield (Y) to the damage cross-section (σ):

$$E = Y / \sigma \qquad \text{Equation 5.3}$$

The secondary ion yield (Y) can be defined by Equation 5.4:

$$Y = N_S / N_p \qquad \text{Equation 5.4}$$

where N_S is the number of secondary ions detected and Np is the total number of applied primary ions.

The damage cross-section and the efficiency of secondary ion formation are useful parameters for comparing the performance of primary ion sources, which can be found in section 5.7.

5.4 Operational modes of SIMS

As discussed previously, there are two different modes to use SIMS investigations including dynamic and static SIMS, which are discussed in more detail here.

5.4.1 Dynamic SIMS

This mode of SIMS implements a constant and continues bombardment of the sample by high primary ion dose (>10^{13} primary ions/cm^2) producing mostly atomic and elemental species. Basically, dynamic SIMS is a highly destructive technique in which many monolayers of samples are quickly sputtered and removed by rastering a high flux of primary ion beam in x and y-direction over a defined area on the sample surface. This creates an etched crater in which the secondary ion signals of specific components are monitored from a certain small area and chemical information is acquired as a function of depth.[153]

In essence, dynamic SIMS and depth profiling are mostly used for analysis of inorganic materials in the semiconductor industry,[154-156] and also highly used in geoscience;[157] however, it has been recently progressed and been developed towards analysis of biological samples such as cells and tissue.[158,159] A high-resolution imaging secondary ion mass spectrometry technique called NanoSIMS has been commercialized, which employs the high energy Cs^+, O^- or O_2^+ primary ion beams to probe the sample at a spot size of several tens of nanometers.[160-162] The technique commonly uses isotopic labeling of the molecules of interest and can provide molecular information from the sample surface offering a potent SIMS based imaging technique at the nano-scale in biological studies.[163-165]

5.4.2 Static SIMS

Static SIMS uses a low primary ion beam current (at 1×10^{13} ions/cm^2 or below) to probe the sample surface and provides molecular information from the uppermost layer of a sample. In this mode, less than 1 % of surface molecules are probed leading to the extremely low probability of impacting the same area twice. Thus, a small amount of secondary ions can be produced under static conditions. As mentioned above, static SIMS allows the analysis of intact molecular species, which is beneficial for the analysis of intact biomolecules from the tissue surface,[88,128] nevertheless, the occurance of low secondary ion signals still challenges SIMS users to increase sensitivity and detection of low concentrations of analytes in complex biological samples. The introduction of the time-of-flight (ToF) mass analyser (described in details in chapter 3) to SIMS in the late 1980s by Benninghoven (1983) and Chait (1981)

provided high ion transmission and detection of a wider mass range, and led to a remarkable increase in the sensitivity.[166,167] The ToF mass analyzer properties have almost satisfied all the requirements for a surface mass spectrometer including detection of all the ions generated, a greatly expanded mass range, and high mass resolution.[168] Further improvements in sensitivity have been also achieved through the development of new primary ion sources and also some specific sample treatments which will be discussed later in this chapter.

5.5 SIMS imaging

SIMS imaging can be performed using either the microscope or the microprobe modes. The microscope mode, which is less common, is equipped with the astigmatic ion optical lens system similar to an optical microscope to produce images following bombardment a large area of the sample surface by a defocused primary ion beam. In this mode, the original spatial position of the desorbed secondary ions is maintained as they travel through the mass analyser and subsequently an image similar to the sample is generated. The spatial resolution is dependent on the instrumental features such as quality of ion optics and the detector but is independent of the beam size.[169]

In the microprobe mode, which is the most common acquisition approach in SIMS imaging, a focused primary ion beam is used to continuously scan a selected area of analysis in the *x* and *y* directions, spot by spot or pixel by pixel. The secondary ions generated are extracted and analyzed separately by the mass analyzer producing a mass spectrum from each pixel and by selecting a specific peak related to a chemical species present in that pixel, the intensity of each of these signals can then be plotted to construct a two dimensional ion image for the particular signal on the sample surface (Figure 5.3). The beam size, which should be within the range of pixel size of the analyzing area, limits and sometimes determines the spatial resolution. [170] If the beam diameter of the primary ion is larger than the pixel size, there is a possibility of over-sampling; as a result, small features of a sample are hard to be highlighted within a sample. But if the spot size is too small, under-sampling occurs in which the pixel might not be accurately representative of the area under analysis.

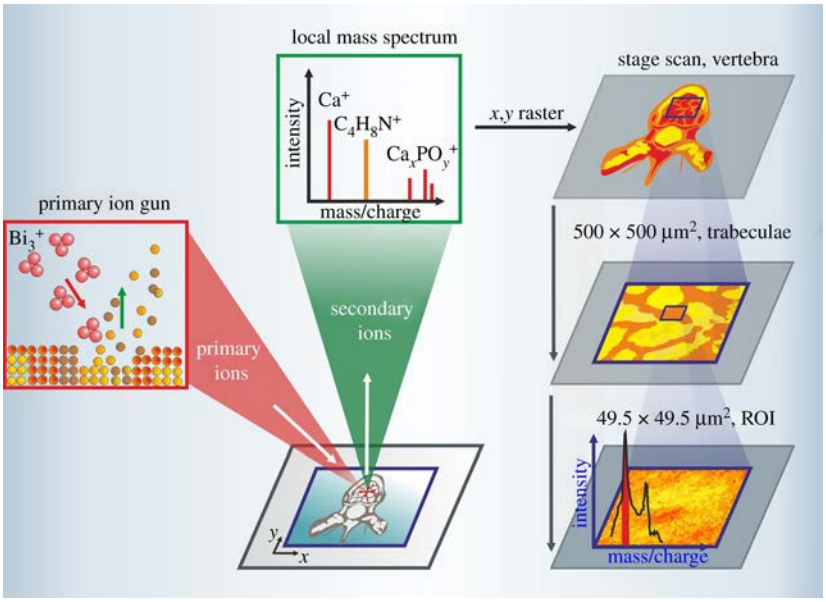

Figure 5.3 Principles and schematic of SIMS imaging in microprobe mode performed on the bone tissue. A focused primary ion beam is used to sputter the sample in a small area called pixel. From each pixel a full mass spectrum is produced. Consequently, an analyte signal from the array of mass spectra is selected and plotted to obtain a 2D ion image for the particular signal representing the distribution of individual molecular ions across the tissue sample. Image reproduced with permission from Henss et al. [171]

5.6 Primary ion sources for SIMS

5.6.1 Liquid Metal Ion Guns (LMIG)

At first, LMIGs were developed and made mainly for microfabrication for many years; gradually their advantages have been explored for SIMS uses as well.[172,173] LMIGs, which produce highly focused ion beams, use a large electric field that is applied to a sharp tip coated with a thin layer of liquid metal inducing the emission of the metal ions. Then ions are generated and extracted from in the form of a Taylor cone and directed in a column (Figure 5.4) creating an extremely focused ion beam stream. This is accurately aimed and deflected to raster the sample surface at specific points called pixels. LMIGs are capable to offer ultrahigh brightness and typical spatial resolutions as low as about 100 nm in the pulsed mode; however, this number should continue to be made smaller by utilizing the most recent instrumental developments.[174,175] The most common LMIGs are Ga^+, In^+, Au_n^+ (n=1, 3) and Bi_n^+ (n=1, 3, 5, 7 as well as Bi_3^{++}). However, monoatomic primary ion sources which have been successfully used for the analysis of biochemicals in biological samples,[176,177] still suffer from the lack of molecular information. The reason for that is when a monoatomic projectile

strikes a sample; it penetrates deep below the sublayers of surface leading to higher fragmentation of molecules in sub-surface layers by breaking intramolecular bonds. In contrast, when metal cluster ions hit a surface, they deposit energy nearer to the surface resulting in smaller damage and also they break into their constituent atoms creating overlapping collision cascades. This leads to multiple sputtering, high interaction and high ion yield events as shown with molecular dynamic simulations by Delcorte and Garrison in.[178]

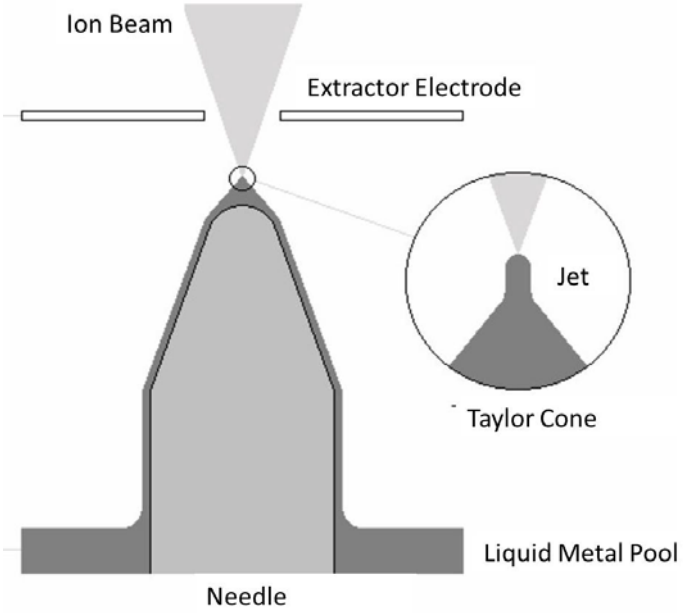

Figure 5.4 Schematic depiction of the principle of the liquid metal ion gun. A Taylor cone is formed by applying an electric field on a small tip of ion gun. Image reproduced with permission from Seifert. [179]

5.6.2 Electron Impact (EI) Sources

In comparison with LMIGs in which only ions from metals that make a liquid coating on a tip are typically used; electron impact (EI) primary ion guns are more flexible and any atom or molecule with the ability to be ionized by electron bombardment in the gas phase can be utilized. Thus, there are typically a variety EI sources ranging from ions of simple gases such as Ar^+ and O_2^+ to more advanced sources including C_{60}^+ and GCIB of Ar_n^+, [174,180] $(H_2O)_n^+$, [181] and $(CO_2)_n^+$. [182] In the Ar GCIB source (Figure 5.5), giant cluster ions of Ar are generated in a supersonic expansion taking place through a small nozzle aperture that shapes the gas flow and forms a jet of clusters. The high-pressure region, which is necessarily applied on gas-phase atoms of Ar to expand and then condense them into the clusters, is separated from the

vacuum stage using a skimmer between the nozzle and electron impact ionization chamber. In the C_{60} source, a solid C_{60} material is heated and facilitates the formation of gas-phase C_{60} molecules that then form C_{60}^+ ions by electron bombardment. [174]

The C_{60} source has high efficiency[183,184] and has been employed to successfully depth profile organic films[185] and biomolecular samples.[158,186] In a dual-beam approach, C_{60} has been also used for sputtering while analysis was performed using a LMIG [187] as an approach that has been successfully applied to biology and for 3D profiling of cells and tissue. [188,189] C_{60} is also able to do both sputtering and analysis in one experiment.[190] However, more recently, massive GCIB argon sources with a larger amount of sputtered materials and also less accumulation of the chemical background noise compared to C_{60} are being progressively used in the experiments.[191-193]

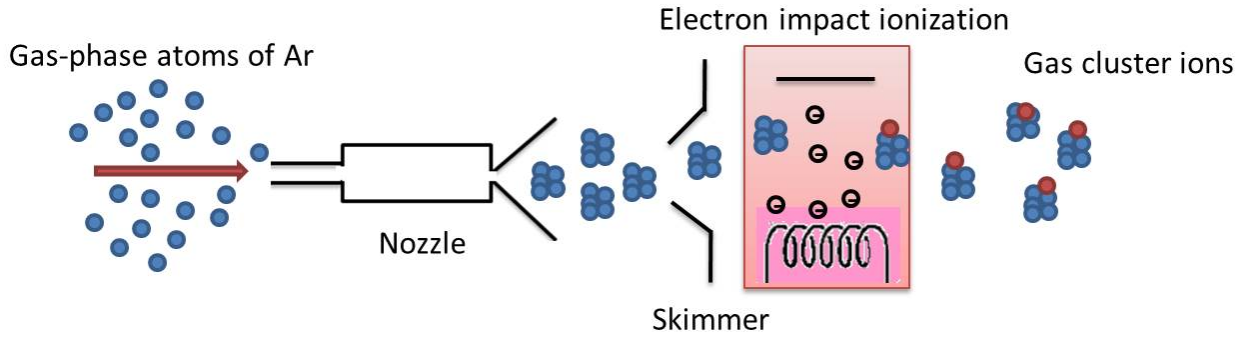

Figure 5.5 Schematic illustration of Ar gas cluster ion beam. The Ar clusters are generated when a high-pressure gas expands into a vacuum through a nozzle facilitating the formation of a jet of clusters.

5.7 Comparison of primary ion sources

The comparison of performance of several monatomic (Ga^+, Cs^+, Au^+) and polyatomic primary ion sources (Au_2^+, Au_3^+, SF_5^+, C_{60}^+) done by Kersting et al. has shown that heavier monatomic primary ions have more efficient secondary ion generation (for an explanation of efficiency see Equation 5.3) than lighter ions in the source, whereas all polyatomic ion sources are more efficient than any of monatomic primary ion sources.[184]

Another study, which was performed by Kollmer,[194] compared the secondary ion emission behaviour caused by bombarding organic and pharmaceutical samples with of a variety of the

atomic and polyatomic ion sources including Ga^+, Au_n^+, Bi_n^+, C_{60}^+. The major conclusions were that the secondary ion yield was significantly increased from atomic Ga^+ to Au^+ and finally to polyatomic C_{60}^+. Based on the results in this study, C_{60}^+ was concluded to have the highest efficiency to produce secondary ions.

Touboul et al.[195] compared the performance of Bi_n^+ and Au_n^+ ion beams on the rat brain samples. They examined different size clusters from the same material and also similar cluster sizes from different projectiles. A significant increase of secondary ion yield efficiency occurred from Bi^+ to Bi_3^+. Moreover, same size and mass of cluster ion beams such as Au_3^+ and Bi_3^+ provided similar properties including secondary ion yields, damage cross sections, efficiencies, and also proper spatial resolution for imaging across brain tissue samples. However, Bi_n^+ had higher beam current than the Au_n^+ beam as a function of cluster size in similar experiment leading to shorter imaging acquisition times. In total, the Bi_n^+ beam was preferred by the authors to the gold LMIG as a primary ion source for high spatial resolution biological imaging with static SIMS owing to its proper spot size, secondary ion yield, and faster analysis time.

Another key primary ion beam is the C_{60}^+ source which provides high secondary ion yield and low damage cross section. Furthermore, the spot size of the C_{60}^+ beam is typically ~1 μm; however, Fletcher et al. reported a sub-200 nm spot size using a C_{60}^+ primary ion source.[196]

In another study recently done by the Fletcher group, the performances of 40 keV C_{60}^+, 20 keV Ar_{4000}^+, and 40 keV Ar_{4000}^+ GCIB guns have been compared on brain tissues and human hair samples. They found that the 40 keV Ar_{4000}^+ source yielded the highest signal compared to the other guns and also the spatial resolution was less than 3 μm. In total, GCIB sources compared to the other guns used to date appear to be highly useful as potential primary ion beams which can be used for both analysis and etching and also they are beneficial to imaging lipid and lipid related compounds in biological samples.[180]

5.8 Technical improvements of SIMS for biological analysis

Apart from the ability of SIMS as a promising analytical technique in analysis of many organic, polymeric and biomolecular species, it still suffers from a high level of fragmentation for small molecules and low ion yield for higher mass molecules. [87,128,197] However, the modern generation of SIMS instruments using polyatomic and cluster primary ion sources such as C_{60}, SF_5, Bi_n, Au_n, Cs_n, and Ar_{4000} have been able to successfully extend the

applicability of SIMS for intact secondary ions of larger species and to effectively improve the performance of SIMS particularly in biological fields. [180,198-201]

To enhance molecular ion yield enabling the use of conventional SIMS for intact biomolecules analysis, some surface modification methods have been developed. One of them is metal assisted-SIMS (MetA-SIMS) proposed by Delcorte et al.[202] in which a thin layer of a noble metal such as silver, gold or platinum is deposited on the sample surface by thermal evaporation or using sputtering-coating. It has been clearly illustrated to increase the production of intact biomolecules (<5 kDa) such as fatty acids, lipids, and peptides in SIMS experiments.[202-205] And also it allows molecular information to be obtained from biological tissue even when using monoatomic ion sources.[206]

Another way to modify the bio-organic surface is matrix-enhanced secondary ion mass spectrometry (ME-SIMS). ME-SIMS can be regarded as a combination of MALDI and SIMS in which the surface of the sample is coated by a thin layer of small molecule organic matrices in similar ways used for MALDI analysis. Two main advantages of this method are its low cost and ease of use. [87,128] A successful use of the MALDI sample preparation protocol in SIMS experiment was reported by Wu and Odom in 1996 when they showed significant enhancement in the yield of intact molecular species.[207] A few years later, many studies on ME-SIMS successfully revealed the ability of this technique to enhance the signals of high mass molecules in the range 1-15 kDa including proteins, peptides, lipids, polymers and organic dyes.[208-213] Also, results with biological tissue studies using ME-SIMS,[214-218] showed significant improvement in the sensitivity and molecular yields of high mass species (m/z ≥2500) enabling SIMS for the study of subcellular distributions of analytes across the tissue sections which is difficult for standard SIMS.[87,214]

Sjövall et al. presented a specific sample modification method in which an imprint of a biological sample was made on a silver surface prior to SIMS analysis. The results showed a significant ion yield enhancement. This method could successfully be used to identify and image the lipid species across the cell membrane in single cells at a spatial resolution less than 0.5 micron using a monoatomic primary ion beam.[219]

Another approach in this regard is the application of Trifluoracetic acid (TFA), which is commonly added to MALDI matrices to assist ionization. Some studies revealed a significant signal enhancement in SIMS when they applied a dilute TFA solution to the surface of samples of polyurethanes [220] and insulin.[221] The Winograd group also determined the

molecular weight of small peptides in femtomole quantities bound to the surfaces of polystyrene beads when the samples were exposed to TFA vapor prior to SIMS analysis. The TFA was used here to break the bond between the polystyrene beads and peptide coatings which led to improvement in the molecular ion signals of covalently bounded species.[222] Also, the application of spraying or inkjet printing of TFA solution to enhance peptide and protein signals in SIMS has been recently reported.[223-225]

5.9 SIMS data analysis

A typical mass spectrum obtained from SIMS analysis contains hundreds of peaks with different intensities based on the chemical composition and structural properties of the sample surface being analyzed. Therefore, SIMS data are intrinsically highly detailed and complex. The complexity and variety of SIMS data can be exacerbated by the use of biological samples most of which are multicomponent and complex in their natures. Additional challenges then result from an enormous SIMS dataset containing multiple spectra originating from multiple samples. To reduce this complexity and dimensionality of SIMS data sets, numerous statistical analysis techniques are being developed among which multivariate analyses (MVA) techniques have to date proved to be the most successful methods aiding interpretation and processing of SIMS datasets without adding human bias.[226,227]

Among the MVA techniques, PCA is the most popular method, which is commonly used in SIMS data analysis to put the data into a comprehensible format. PCA essentially reduces the complexity and simplifies the dataset without loss of information. This method discriminates similarities and differences in SIMS spectra and classifies spectra into groups. PCA is a variant of factor analysis that decreases the number of observations of possibly correlated variables (the peaks in m/z values in SIMS spectra) from many hundreds to smaller values of linearly uncorrelated variables called principal components where the first principal component (PC1) captures the greatest variance in the dataset and each succeeding component expresses the remaining variance. The outputs of PCA are the scores and loadings plots which display separation of different groups of samples and the variables causing the group separation, respectively.[226,228]

Another MVA method is orthogonal partial least squares discriminant analysis (OPLS-DA), which is a classification and grouping approach relying on a projection of samples as PCA

does. OPLS-DA has been recently presented and thus far successfully performed on SIMS data to discriminate and examine chemical differences between two groups.[229-231] Briefly, this method is able to discriminate and separate predictive (known) variances presenting the discrimination between groups from non-predictive (orthogonal) variances showing differences within the groups and it can exclusively focus on the effect of interest which might be covered by unwanted variations.[229,230,232] In this thesis, both PCA and OPLS-DA were successfully used to treat the SIMS data providing valuable results shown in several papers.

Summary of Papers

The main aim of this thesis has been to probe, analyze and image lipid compounds across biological samples by use of MSI techniques including SIMS and MALDI imaging. The samples used in the thesis were brain and intestine tissue sections from rodent models as well as fruit fly brain sections. This thesis can be divided into two units. In the first part including papers I, II and V, different sample modification methods for SIMS (papers I and V) and MALDI (paper II) have been examined with the aim to improve the information acquired for a variety of the lipid components. Also, the possible mechanisms have been investigated. The second section, which includes papers III and IV, is a general investigation and application of SIMS for lipid analysis on tissue samples. Following is a short summary of each of the five papers that make up the body of the thesis.

Despite the promising ability of the SIMS technique for the analysis of biomolecular species, it still suffers from high fragmentation for small molecules and low ion yield for higher mass molecules. One possible remedy in this regard is ME-SIMS, which is a common surface modification method to improve intact ion yield and sensitivity in conventional SIMS. In **paper I**, the possible mechanism underlying the ion yield enhancement in ME-SIMS using a solvent-free deposition method has been characterized. I utilized sublimation to deposit a thin layer of DHB, a conventional MALDI matrix, on the surface of rat brain cerebellum tissue sections. Then samples were exposed to SIMS analysis using a Bi cluster ion gun as a primary ion source. Additionally, scanning electron microscopy (SEM) was used to evaluate the deposited matrix layer, which confirmed the quality and coverage of the sublimed DHB layer on the samples. To assess lipid changes here, data acquired from untreated and DHB sublimed samples analyzed with SIMS were compared using PCA for the white and grey matter separately. Results illustrated a significant enhancement of ion yields for a multitude of lipid species in the higher mass region (specifically in the range of 700-950 m/z) and also a major reduction of cholesterol signals in the sublimed tissue samples for both grey and white matter. The fact that enhancement was observed for both protonated and non-protonated species as well as Na- and K-adduct species, supports the hypothesis that the enhancement is not caused by direct proton donation in the solid or gaseous phases. Rather it is derived by removal or suppression of the cholesterol crystals from the surface of the sample, which allows other species to be detected more readily. It is also possible that the extraction of some specific

lipids into the deposited matrix directly leads to an increase of higher mass lipid ion yield. In addition, images acquired in this work indicated that matrix deposition doesn't influence the spatial resolution, which is retained around 2 μm.

In **paper II**, various lipid species and their spatial distribution in fruit fly brain sections were detected and investigated using laser desorption ionization (LDI). In this work, prior to analysis, fly brain sections were treated with two different methods including sublimation (as a solvent-free matrix deposition technique) and gold (Au) nanoparticles with a "spray-on" deposition. Sublimation was used to deposit two different organic matrices, DHB and CHCA on the samples. The samples were also modified with trifluoroacetic acid (TFA) vapor exposure, causing recrystallization of the matrix. This recrystallization enhances the incorporation of analytes into the matrix leading to higher ionization efficiency. These sample preparation methods in comparison showed different abilities for lipid molecular ion detection and imaging and therefore they can be combined to provide complementary information for a specific group of lipid species including diacylglycerides, phosphatidylcholines, and triacylglycerides. Furthermore, ion images with enhanced contrast and more spatial details could be achieved using deposition of Au nanoparticles, and this is a potent technique for cellular and subcellular imaging. Development of different sample modification approaches here with both MALDI and SALDI offers the best and most varieties of lipid chemical images of the fly brain so far with LDI.

In **paper III**, SIMS imaging using a Bi-cluster ion source was used to study possible changes in the lipid cell membrane across intestine tissue samples from rats fed specially processed cereals (SPC) compared to control rats fed ordinary diet. This cereal is known to help the activity of antisecretory factor (AF), an endogenous protein with proven regulatory effect on the hyper-fluid secretion and inflammation decreasing some intestinal symptoms in inflammatory bowel disease. To date, the exact mechanism for the AF activation process at the cellular level is unknown. In this work, to achieve insight into the possible mechanisms involved, SIMS analysis was performed to track food-induced alterations in the lipid composition of intestinal tissue sections from two groups of control and SPC-fed animals. SIMS data were then subjected to OPLS-DA data analysis, which was used to discriminate and differentiate between the two groups. The significant changes in lipid content, particularly in vitamin E, phospholipids, and phosphosphingolipids that were observed here, indicates the lipids might be directly associated with the working mechanism of an SPC-induced AF activation in intestinal tissue.

Some studies have shown the effect of an SPC diet on the activation of AF in the brain, leading to a decrease of intracranial pressure (ICP). In **paper IV**, I continued to study and compare the lipid content of cell membranes in brain sections of rat exposed to an SPC diet with control rats fed a normal diet. In this paper, I used SIMS imaging equipped with a Bi cluster ion source to analysis the lipid composition of the brain section samples. PCA data analysis was performed on the SIMS data to differentiate and discriminate between the two groups. Results illustrated significant changes for some lipid species including cholesterol, vitamin E, phosphatidylcholine (PC), phosphatidylethanolamine (PE), phosphinothricin, and fatty acids such as palmitic and oleic acid between the control and the SPC-fed group. The changes of lipid components in the brain following SPC feeding, which were observed here, might provide insight into the working mechanisms for AF activation in the brain.

In paper V, I investigated a sample treatment method to increase the detectable mass range of SIMS, which is critical for biological analysis. SIMS imaging can provide ion images with high spatial showing the intensity distribution of detected chemicals but is often restricted to low mass species which is a notable disadvantage for SIMS. In this paper, rat brain cerebellum tissue sections were analyzed. It was demonstrated that applying GCIBs as a primary ion source in combination with sample pretreatment with TFA vapor exposure could significantly enhance the mass range for intact biomolecular imaging. Additionally, different exposure times were investigated in order to obtain the optimum TFA treatment conditions for enhancing the high mass signals as well as detecting new species in the mass spectrum that previously could not be observed. TFA removes the cholesterol enrichment and crystals at the surface of white matter in the brain sections and thus a wide range of lipid species are uncovered to be ionized and detected by SIMS. This sample pretreatment proved to be able to expand the potential detectable mass range of SIMS analysis for neurological studies. This technical improvement enables high molecular mass imaging at high spatial resolutions closing the gap between SIMS and MALDI.

Concluding Remarks

In this thesis, specific sample treatments were developed to improve sensitivity and intact ion yields in SIMS and as a part of possible mechanisms involved in this enhancement, removing cholesterol crystals from the sample surface to allow detection of other species has been suggested. In addition, to investigate the biological application of SIMS, I have shown that we SIMS imaging can be successfully applied to analyze the lipid content of cell membranes in the brain and intestinal tissue sections from rats fed a special, SPC, diet. The results indicated significant alteration in lipid composition of the cell membrane in response to this food intake suggesting a lipid and cell membrane involvement in the activating of AF protein.

Also, I developed an alternative imaging technique using nanoparticle LDI-MS with gold nanoparticles deposited on fruit fly brain samples. Also, comparison of different matrices using different deposition methods showed that the type of lipid species detected in each method depends on the strategy of sample preparation as well as the type of material used. I conclude that each method can be used in a complementary approach to detect a variety of lipid species.

In conclusion, technological improvements, innovations, and the results presented in this thesis offer great potential to utilize MSI more efficiently in further lipid studies. Access to higher mass ranges and higher yields of intact biomolecules can open the doors to better understand the mechanisms of diseases that involve lipids and help find possible treatments.

Acknowledgements

If you ask me about my time as a PhD student, I would say that it is the time given to you as an amazing gift to realize that despite all challenges, difficulties and failures, you must keep going forward and definitely one day you will make it. Though, this would not be possible without many people who helped and supported you technically, mentally, and spiritually on this road. Now I'm so delighted to find this chance to acknowledge some of this people who are so important to me to MAKE IT.

I would first like to thank my main supervisor, **Professor Andrew Ewing**, for believing in me, accepting me, and giving me this opportunity to do my PhD study in your research group. I am forever grateful for your excellent scientific guidance, kind help and truly reliable support. I am so thankful for your incredible knowledge and expertise provided to me with an opportunity to grow up in science. Thank you, Andy, for making a positive and friendly group environment where everybody is respected and where science is challenging yet fun. Also, thank you for all amazing social activities that you involved us in, making a great time for me to enjoy with my friends and colleagues that I will never forget.

My second supervisor, **Dr. Per Malmberg**, for being supportive and encouraging to me during my PhD. Thank you, Per for your patience and nice help in teaching me and providing me with an insight into instrumentation at the start. Also, thank you for being available for constructive and valuable discussions and for your immense guidance, which allowed me to accomplish exciting and interesting projects during my PhD studies. Thank you for your positive, respectful, and nice attitude.

Also, I would like to acknowledge **Dr. John Fletcher** who was always helpful when I had scientific questions. Thank you, John, for your nice advice and scientific discussions.

My great co-authors of the papers, **Nhu Phan**, **Amir Mohammadi**, **Tina Angerer** and **Lin Ren**, thank you all for your kind help, scientific discussions and nice contributions. It was wonderful to work with you guys and I learnt a lot from all of you. I wish you all the best in your research and your life. Also, I was very fortunate to work with two great medical doctors at the Sahlgrenska; **Eva Jennische** and **Stefan Lange**. I appreciate your remarkable biological

knowledge and expertise. Thanks to both of you for sharing your very valuable scientific experiences with me.

During my PhD study, I was also assigned to teach and help undergraduate students in the lab. It was the sweetest assignment that I have ever had, as I love teaching, and when I have even a small portion of what others learn making me unbelievably delighted. Some people made this experience even more exciting with their nice help and support. I would like to acknowledge **Ann-Sofie Cans** and **Aldo Jesorka** as teaching course coordinators who always kindly provided me with excellent technical help and nice support. I would also like to thank **Lynga Normann** and **Sara Costa** for a constant supply of materials and for your very nice organization in the lab that helped me give a better teaching job.

I wish to thank **Per Lincoln** for your incredibly kind attention and your supportive help whenever I needed it.

The nice ladies from the administration, **Gunilla Saethe**, **Carina Pettersson**, **Lotta Pettersson** and **Anna Molander** who were always ready to provide me with their kind help, thank you all for your incredibly nice organization and truly nice help.

I would also like to thank all my friends, colleagues and members in the **Ewing**, **Fletcher**, **Cans** and **Safina** research groups, in the past and present. Thank you for all the discussions in group meetings and social group activities.

A big thank to my dear Tang Soo Do family to accept me and treat me in such a warm and nice manner that I have never seen in any training club. Especially I would like to thank my instructor, **Andy Ewing**, from whom I learned how to be confident, but humble, enthusiastic but patient, creative but respectful to others, and be focused but helpful. Awesome codes of Tang Soo Do truly changed my view to the life, and I found it not only a useful training for the body but also it is a philosophy that has helped me mentally in my life and PhD study.

My friend, **Nhu Phan**, thank you for your friendship, nice attitude, kind help and positive energy. Thank you, Nhu, for many fun and enjoyable times in the lab, Tang Soo Do and groups activities.

All my friends outside of science, thank you, everyone, for all the nice gatherings, fun and joyful times that you made for me.

I would like to express my deep and warm gratitude to my awesome family, my parents and my great sisters who always provide me with an enormous love in its truest and purest form. Thank you all for being in my life to make it more colorful and more meaningful.

At last but not at least to my dearest **Amir**, words cannot express how much you mean in my life. I love you ☺

References

1 Siegel, G. J., Albers, R. W., Brady, S. T. & Price, D. L. Basic Neurochemistry: Molecular, Cellular, and Medical Aspects. *Elsevier Academic Press, Burlington, MA* (2006).

2 Blumenfeld, H. Neuroanatomy through Clinical Cases *Sinauer Associates, Inc., Sunderland, MA* (2010).

3 Savtchenko, L. P. & Rusakov, D. A. The optimal height of the synaptic cleft. *Proc. Natl. Acad. Sci. U. S. A.* **104**, 1823-1828, doi:10.1073/pnas.0606636104 (2007).

4 Herculano-Houzel, S. The human brain in numbers: a linearly scaled-up primate brain. *Front Hum Neurosci* **3**, 1-11, doi:10.3389/neuro.09.031.2009 (2009).

5 Cooper, J., Bloom, F. & Roth, R. The Biochemical Basis of Neuropharmacology,. *Oxford University Press* **eighth edn** (2003).

6 Lodish, H. *et al.* Molecular Cell Biology, Overview of Neuron Structure and Function. *W.H.Freeman & Co Ltd, New York, NY* (2000).

7 Kandel, E. R., Jessell, T. M., Siegelbaum, S. A. & Hudspeth, A. J. Principle of Neural Science. *McGraw-Hill Education* **fifth edn** (2013).

8 Fischbach, G. D. Mind and Brain. *Scientific American* **267**, 48-57 (1992).

9 Miller, D. W., Cookson, M. R. & Dickson, D. W. Glial cell inclusions and the pathogenesis of neurodegenerative diseases. *Neuron Glia Biology* **1**, 13-21, doi:10.1017/S1740925X04000043 (2004).

10 Yong, V. W. *et al.* The promise of minocycline in neurology. *The Lancet Neurology* **3**, 744-751, doi:10.1016/s1474-4422(04)00937-8 (2004).

11 Nithianantharajah, J. & Hannan, A. J. Enriched environments, experience-dependent plasticity and disorders of the nervous system. *Nat Rev Neurosci* **7**, 697-709, doi:10.1038/nrn1970 (2006).

12 Angela Cenci, M., Whishaw, I. Q. & Timothy S. Animal models of neurological deficits: how relevant is the rat? *Neuroscience* **3**, 574-579 (2002).

13 Tsujino, N. & Sakurai, T. Role of orexin in modulating arousal, feeding, and motivation. *Front Behav Neurosci* **7**, 28, doi:10.3389/fnbeh.2013.00028 (2013).

14 Nuñez, A., Rodrigo-Angulo, M., De Andrés, I. & Garzón, M. Hypocretin/Orexin Neuropeptides: Participation in the Control of Sleep-Wakefulness Cycle and Energy Homeostasis. **7**, 50-59, doi:10.2174/157015909787602797 (2009).

15 Ramnani, N. The primate cortico-cerebellar system: anatomy and function. *Nat Rev Neurosci* **7**, 511-522, doi:10.1038/nrn1953 (2006).

16 Glickstein, M. What does the cerebellum really do? *Curr. Biol.* **17**, R824-827, doi:10.1016/j.cub.2007.08.009 (2007).

17 Miquel, M., Toledo, R., Garcia, L., Coria-Avila, G. & Manzo, J. Why Should We Keep the Cerebellum in Mind When Thinking About Addiction? *Current Drug Abuse Reviewse* **2**, 26-40, doi:10.2174/1874473710902010026 (2009).

18 Middleton, F. A. & Strick, P. L. The cerebellum:an overview. *TINS* **21**, 367-369 (1998).

19 Thach, W. T., Goodkin, H. P. & Keating, J. G. The cerebellum and the adaptive coordination of movement. *Annual Review of Neuroscience*, **15**, 403–442 (1992).

20 Strick, P. L., Dum, R. P. & Fiez, J. A. Cerebellum and Nonmotor Function. *Annual Review of Neuroscience* **32**, 413-434, doi:10.1146/annurev.neuro.31.060407.125606 (2009).
21 Xiang, H. *et al.* Involvement of the cerebellum in semantic discrimination: an fMRI study. *Hum Brain Mapp* **18**, 208-214, doi:10.1002/hbm.10095 (2003).
22 Bastian, A. J. Learning to predict the future: the cerebellum adapts feedforward movement control. *Curr. Opin. Neurobiol.* **16**, 645-649, doi:10.1016/j.conb.2006.08.016 (2006).
23 Baumgartner, T., Lutz, K., Schmidt, C. F. & Jancke, L. The emotional power of music: how music enhances the feeling of affective pictures. *Brain Res* **1075**, 151-164, doi:10.1016/j.brainres.2005.12.065 (2006).
24 Sacchetti, B., Baldi, E., Lorenzini, C. A. & Bucherelli, C. Cerebellar role in fear-conditioning consolidation. *Proc. Natl. Acad. Sci. U. S. A.* **99**, 8406-8411, doi:10.1073/pnas.112660399 (2002).
25 Sacchetti, B., Scelfo, B., Tempia, F. & Strata, P. Long-term synaptic changes induced in the cerebellar cortex by fear conditioning. *Neuron* **42**, 973-982, doi:10.1016/j.neuron.2004.05.012 (2004).
26 Schutter, D. J. & van Honk, J. An electrophysiological link between the cerebellum, cognition and emotion: frontal theta EEG activity to single-pulse cerebellar TMS. *Neuroimage* **33**, 1227-1231, doi:10.1016/j.neuroimage.2006.06.055 (2006).
27 Turner, B. M. *et al.* The cerebellum and emotional experience. *Neuropsychologia* **45**, 1331-1341, doi:10.1016/j.neuropsychologia.2006.09.023 (2007).
28 Holstege, G., et al. Brain Activation during Human Male Ejaculation. *The Journal of Neuroscience* **23**, 9185–9193 (2003).
29 Manzo, J. *et al.* Fos expression at the cerebellum following non-contact arousal and mating behavior in male rats. *Physiol Behav* **93**, 357-363, doi:10.1016/j.physbeh.2007.09.005 (2008).
30 Petacchi, A., Laird, A. R., Fox, P. T. & Bower, J. M. Cerebellum and auditory function: an ALE meta-analysis of functional neuroimaging studies. *Hum Brain Mapp* **25**, 118-128, doi:10.1002/hbm.20137 (2005).
31 Bolbecker, A. R., et al. Eyeblink conditioning anomalies in bipolar disorder suggest cerebellar dysfunction. *Bipolar Disorders* **11**, 19–32 (2009).
32 Bolbecker, A. R. *et al.* Exploration of cerebellar-dependent associative learning in schizophrenia: effects of varying and shifting interstimulus interval on eyeblink conditioning. *Behav Neurosci* **125**, 687-698, doi:10.1037/a0025150 (2011).
33 Steinmetz, A. B. & Rice, M. L. Cerebellar-dependent delay eyeblink conditioning in adolescents with Specific Language Impairment. *J Neurodev Disord* **2**, 243-251, doi:10.1007/s11689-010-9058-z (2010).
34 Berglund, E. C. *et al.* Oral administration of methylphenidate blocks the effect of cocaine on uptake at the Drosophila dopamine transporter. *ACS Chem Neurosci* **4**, 566-574, doi:10.1021/cn3002009 (2013).
35 Phan, N. T., Fletcher, J. S. & Ewing, A. G. Lipid structural effects of oral administration of methylphenidate in Drosophila brain by secondary ion mass spectrometry imaging. *Anal Chem* **87**, 4063-4071, doi:10.1021/acs.analchem.5b00555 (2015).
36 Wolf, F. W. & Heberlein, U. Invertebrate models of drug abuse. *J Neurobiol* **54**, 161-178, doi:10.1002/neu.10166 (2003).
37 Kraut, R. Roles of sphingolipids in Drosophila development and disease. *J Neurochem* **116**, 764-778, doi:10.1111/j.1471-4159.2010.07022.x (2011).

38 Keene, A. C. & Waddell, S. Drosophila olfactory memory: single genes to complex neural circuits. *Nat Rev Neurosci* **8**, 341-354, doi:10.1038/nrn2098 (2007).
39 Bernards, A. & Hariharan, I. K. Of flies and men — studying human disease in Drosophila. *Current Opinion in Genetics and Development* **11**, 274–278 (2001).
40 Pandey, U. B. & Nichols, C. D. Human disease models in Drosophila melanogaster and the role of the fly in therapeutic drug discovery. *Pharmacol Rev* **63**, 411-436, doi:10.1124/pr.110.003293 (2011).
41 Atkins, M. & Mardon, G. Signaling in the third dimension: the peripodial epithelium in eye disc development. *Dev Dyn* **238**, 2139-2148, doi:10.1002/dvdy.22034 (2009).
42 Heisenberg, M. Fly Brains. *John Wiley & Sons, Ltd* (2001).
43 Wolff, T., Iyer, N. A. & Rubin, G. M. Neuroarchitecture and neuroanatomy of the Drosophila central complex: A GAL4-based dissection of protocerebral bridge neurons and circuits. *J Comp Neurol* **523**, 997-1037, doi:10.1002/cne.23705 (2015).
44 Hanesch, U., Fischbach, K. F. & Heisenberg, M. Neuronal architecture of the central complex in Drosophila melanogaster. *Cell Tissue Res* **257**, 343-366 (1989).
45 Tanaka, N. K., Endo, K. & Ito, K. Organization of antennal lobe-associated neurons in adult Drosophila melanogaster brain. *J Comp Neurol* **520**, 4067-4130, doi:10.1002/cne.23142 (2012).
46 Stocker, R. F. & Schorderet, M. Cobalt Filling of Sensory Projections from Internal and External Mouthparts in Drosophila. *Cell Tissue Res* **216**, 513-523 (1981).
47 Nichols, C. D. Drosophila melanogaster neurobiology, neuropharmacology, and how the fly can inform central nervous system drug discovery. *Pharmacol Ther* **112**, 677-700, doi:10.1016/j.pharmthera.2006.05.012 (2006).
48 Alberts, B. *et al.* Molecular biology of the cell. *New York: Garland Science* **forth edn** (2002).
49 Meer, G. V., Voelker, D. R. & Feigenson, G. W. Membrane lipids: where they are and how they behave. *Nat Rev Mol Cell Biol* **9**, 112-124, doi:10.1038/nrm2330 (2008).
50 Jones, J. J., Stump, M. J., Fleming, R. C., Lay, J. O., Jr. & Wilkins, C. L. Strategies and data analysis techniques for lipid and phospholipid chemistry elucidation by intact cell MALDI-FTMS. *J Am Soc Mass Spectrom* **15**, 1665-1674, doi:10.1016/j.jasms.2004.08.007 (2004).
51 Marieb, E. N. E. & Hoehn, K. H. Anatomy & Physiology. *Cell Structure and Function*, San Francisco Pearson Benjamin Cummings (2006).
52 Fahy, E., Cotter, D., Sud, M. & Subramaniam, S. Lipid classification, structures and tools. *Biochimica et biophysica acta* **1811**, 637-647, doi:10.1016/j.bbalip.2011.06.009 (2011).
53 Or-Rashid, M. M., Odongo, N. E. & McBride, B. W. Fatty acid composition of ruminal bacteria and protozoa, with emphasis on conjugated linoleic acid, vaccenic acid, and odd-chain and branched-chain fatty acids. *J Anim Sci* **85**, 1228-1234, doi:10.2527/jas.2006-385 (2007).
54 Berg, J. M., Tymoczko, J. L. & Stryer, L. Triacylglycerols Are Highly Concentrated Energy Stores. *W H Freeman,New York,* **fifth edn** (2002).
55 Schnaar, R. L., Suzuki, A. & Stanley, P. Essentials of Glycobiology, Glycosphingolipids. *Cold Spring Harbor, New York, NY*, (2009).
56 Farooqui, A. A., Horrocks , L. A. & Farooqui, T. Glycerophospholipids in brain: their metabolism, incorporation into membranes, functions, and involvement in neurological disorders. *Chemistry and Physics of Lipids* **106**, 1–29 (2000).

57 Piomelli, D., Astarita, G. & Rapaka, R. A neuroscientist's guide to lipidomics. *Nat Rev Neurosci* **8**, 743-754, doi:10.1038/nrn2233 (2007).
58 Al-Saad, K. A., Siems, W. F., Hill, H. H., Zabrouskov, V. & Knowles, N. R. Structural analysis of phosphatidylcholines by post-source decay matrix-assisted laser desorption/ionization time-of-flight mass spectrometry. *J Am Soc Mass Spectrom* **14**, 373-382, doi:10.1016/S1044-0305(03)00068-0 (2003).
59 Patel, D. & Witt, S. N. Ethanolamine and Phosphatidylethanolamine: Partners in Health and Disease. *Oxid Med Cell Longev* **2017**, 1-18, doi:10.1155/2017/4829180 (2017).
60 Murphy, R. C. & Axelsen, P. H. Mass spectrometric analysis of long-chain lipids. *Mass Spectrom Rev* **30**, 579-599, doi:10.1002/mas.20284 (2011).
61 Fadeel, B. & Xue, D. The ins and outs of phospholipid asymmetry in the plasma membrane: roles in health and disease. *Crit Rev Biochem Mol Biol* **44**, 264-277, doi:10.1080/10409230903193307 (2009).
62 Lee, S. H., Meng, X. W., Flatten, K. S., Loegering, D. A. & Kaufmann, S. H. Phosphatidylserine exposure during apoptosis reflects bidirectional trafficking between plasma membrane and cytoplasm. *Cell Death Differ* **20**, 64-76, doi:10.1038/cdd.2012.93 (2013).
63 D'Souza, K. & Epand, R. M. Enrichment of phosphatidylinositols with specific acyl chains. *Biochim Biophys Acta* **1838**, 1501-1508, doi:10.1016/j.bbamem.2013.10.003 (2014).
64 Hsu, F. F. & Turk, J. Studies on Phosphatidylglycerol with Triple Quadrupole Tandem Mass Spectrometry with Electrospray Ionization: Fragmentation Processes and Structural Characterization. *J Am Soc Mass Spectrom* **12**, 1036–1043 (2001).
65 Gault, C. R., Obeid, L. M. & Hannun, Y. A. An overview of sphingolipid metabolism: from synthesis to breakdown. *Adv Exp Med Biol.* **688**, 1-23 (2010).
66 Jana, A. & Pahan, K. Sphingolipids in multiple sclerosis. *Neuromolecular Med* **12**, 351-361, doi:10.1007/s12017-010-8128-4 (2010).
67 Slotte, J. P. & Ramstedt, B. The functional role of sphingomyelin in cell membranes. *European Journal of Lipid Science and Technology* **109**, 977-981, doi:10.1002/ejlt.200700024 (2007).
68 Robert K. Yu, Yi-Tzang Tsai, Toshio Ariga & Yanagisawa, M. Structures, biosynthesis, and functions of gangliosides. *J Oleo Sci.* **60**, 537–544 (2011).
69 Simons, K. & Ehehalt, R. Cholesterol, lipid rafts, and disease. *Journal of Clinical Investigation* **110**, 597-603, doi:10.1172/jci0216390 (2002).
70 Orth, M. & Bellosta, S. Cholesterol: its regulation and role in central nervous system disorders. *Cholesterol* **2012**, 1-19, doi:10.1155/2012/292598 (2012).
71 Simons, K. & Ikonen, E. Functional rafts in cellmembranes. *Nature* **387**, 569-572 (1997).
72 Khan, W. A., Blobet, G. C. & Hannun, Y. A. Arachidonic Acid and Free Fatty Acids as Second Messengers and the Role of Protein Kinase C. *Cellular Signalling* **7**, 171-184 (1995).
73 Lawrence W. Fitzgerald, Jordi Ortiz, Azita G. Hamedani & Nestler, a. E. J. Drugs of Abuse and Stress Increase the Expression of GluR1 and NMDAR1 Glutamate Receptor Subunits in the Rat Ventral Tegmental Area: Common Adaptations among Cross-Sensitizing Agents. *The Journal of Neuroscience,* **76**, 274-282 (1996).

74 Buccoliero, R. The roles of ceramide and complex sphingolipids in neuronal cell function. *Pharmacological Research* **47**, 409-419, doi:10.1016/s1043-6618(03)00049-5 (2003).
75 Ohanian, J., G Liu, V Ohanian & Heagerty, A. M. Lipid second messengers derived from glycerolipids and sphingolipids, and their role in smooth musclefunction. *Acta Physiol Scand* **164**, 533-548 (1998).

76 O ’brien, J. S. & Sampson, J. S. Lipid composition of the normal human brain: gray matter, white matter, and myelin. *JOURNAL OF LIPID RESEARCH* **6**, 537-544 (1965).

77 Adibhatla, R. M. & Hatcher, J. F. Role of Lipids in Brain Injury and Diseases. *Future Lipidol* **2**, 403–422 (2007).
78 Lim, W. L., Martins, I. J. & Martins, R. N. The involvement of lipids in Alzheimer's disease. *J Genet Genomics* **41**, 261-274, doi:10.1016/j.jgg.2014.04.003 (2014).
79 Farooqui, A. A., Ong, W. Y. & Horrocks, L. A. Biochemical Aspects of Neurodegeneration in Human Brain: Involvement of Neural Membrane Phospholipids and Phospholipases A2. *Neurochemical Research* **29**, 1961–1977 (2004).

80 Hwang, O. Role of oxidative stress in Parkinson's disease. *Exp Neurobiol* **22**, 11-17, doi:10.5607/en.2013.22.1.11 (2013).
81 Blesa, J., Trigo-Damas, I., Quiroga-Varela, A. & Jackson-Lewis, V. R. Oxidative stress and Parkinson's disease. *Front Neuroanat* **9**, 1-9, doi:10.3389/fnana.2015.00091 (2015).
82 Schwarz, E., et al., & High Throughput Lipidomic Profiling of Schizophrenia and Bipolar Disorder Brain Tissue Reveals Alterations of Free Fatty Acids, Phosphatidylcholines, and Ceramides. *Journal of Proteome Research* **7**, 4266–4277 (2008).

83 Kaddurah-Daouk, R. *et al.* Impaired plasmalogens in patients with schizophrenia. *Psychiatry Res* **198**, 347-352, doi:10.1016/j.psychres.2012.02.019 (2012).
84 Solberg, D. K., Bentsen, H., Refsum, H. & Andreassen, O. A. Lipid profiles in schizophrenia associated with clinical traits: a five year follow-up study. *BMC Psychiatry* **16**, 1-9, doi:10.1186/s12888-016-1006-3 (2016).
85 Lipton, P. Ischemic Cell Death in Brain Neurons. *PHYSIOLOGICAL REVIEWS* **79**, 1431–1568 (1999).
86 Shanta, S. R. *et al.* Global changes in phospholipids identified by MALDI MS in rats with focal cerebral ischemia. *J Lipid Res* **53**, 1823-1831, doi:10.1194/jlr.M022558 (2012).
87 Chughtai, K. & Heeren, R. M. A. Mass Spectrometric Imaging for Biomedical Tissue Analysis. *Chem. Rev.* **110**, 3237–3277 (2010).
88 McDonnell, L. A. & Heeren, R. M. Imaging mass spectrometry. *Mass Spectrom Rev* **26**, 606-643, doi:10.1002/mas.20124 (2007).
89 Zimmerman, T. A., Monroe, E. B., Tucker, K. R., Rubakhin, S. S. & Sweedler, J. V. Chapter 13 Imaging of Cells and Tissues with Mass Spectrometry. **89**, 361-390, doi:10.1016/s0091-679x(08)00613-4 (2008).
90 Dass, C. & Fundamentals of Contemporary Mass Spectrometry. *John Wiley & Sons, Inc., Hoboken, NJ, USA*, 608 pages (2007).
91 Hoffmann. E.D. & Stroobant. V. Mass Spectrometry Principles and Applications,. *Wiley Interscience, Hoboken, NJ,* , 502 pages (2007).

92 Yates, J. R. A century of mass spectrometry: from atoms to proteomes. *Nature Methods* **8**, 633-637, doi:10.1038/nmeth.1659 (2011).
93 Griffith, J. A Brief History of Mass Spectrometry. *Anal. Chem.* **80**, 5678–5683 (2008).
94 Stephens, W. E. A pulsed mass spectrometer with time dispersion. *Phys Rev* **69**, 616-618 (1946).
95 Mamyrin, B. A. Time-of-flight mass spectrometry (concepts, achievements, and prospects). *International Journal of Mass Spectrometry* **206**, 251–266 (2001).
96 Standing, K. G. Timing the flight of biomolecules: a personal perspective. *International Journal of Mass Spectrometry* **200**, 597–610 (2000).
97 Mamyrin, B. A. Laser Assisted Reflectron Time-of-Flight Mass Spectrometry. *International Journal of Mass Spectrometry and Ion Processes* **131**, 1-19 (1994).
98 Karas, M. Time-of-Flight Mass Spectrometer with Improved Resolution. *J. Mass Spectrom* **32**, 1-3 (1997).
99 Mamyrin, B. A., Karataev, V. I., Shmikk, D. V. & Zagulin, V. A. The mass-reflectron, a new nonmagnetic time-of-flight mass spectrometer with high resolution. *SOy. Phys.·JETP* **37** 45-48 (1973).
100 Greer, T., Sturm, R. & Li, L. Mass spectrometry imaging for drugs and metabolites. *J Proteomics* **74**, 2617-2631, doi:10.1016/j.jprot.2011.03.032 (2011).
101 Northen, T. R. *et al.* Clathrate nanostructures for mass spectrometry. *Nature* **449**, 1033-1036, doi:10.1038/nature06195 (2007).
102 Guenther, S., Römpp, A., Kummer, W. & Spengler, B. AP-MALDI imaging of neuropeptides in mouse pituitary gland with 5µm spatial resolution and high mass accuracy. *International Journal of Mass Spectrometry* **305**, 228-237, doi:10.1016/j.ijms.2010.11.011 (2011).
103 Yang, J. & Caprioli, R. M. Matrix sublimation/recrystallization for imaging proteins by mass spectrometry at high spatial resolution. *Anal Chem* **83**, 5728-5734, doi:10.1021/ac200998a (2011).
104 Fletcher, J. S. & Vickerman, J. C. A new SIMS paradigm for 2D and 3D molecular imaging of bio-systems. *Anal Bioanal Chem* **396**, 85-104, doi:10.1007/s00216-009-2986-3 (2010).
105 Sjövall, P., Lausmaa, J. & Johansson, B. Mass Spectrometric Imaging of Lipids in Brain Tissue. *Anal Chem* **76**, 4271-4278 (2004).
106 Taban, I. M. *et al.* Imaging of peptides in the rat brain using MALDI-FTICR mass spectrometry. *J Am Soc Mass Spectrom* **18**, 145-151, doi:10.1016/j.jasms.2006.09.017 (2007).
107 Lanni, E. J., Rubakhin, S. S. & Sweedler, J. V. Mass spectrometry imaging and profiling of single cells. *J Proteomics* **75**, 5036-5051, doi:10.1016/j.jprot.2012.03.017 (2012).
108 Amstalden van Hove, E. R., Smith, D. F. & Heeren, R. M. A concise review of mass spectrometry imaging. *J Chromatogr A* **1217**, 3946-3954, doi:10.1016/j.chroma.2010.01.033 (2010).
109 Passarelli, M. K. & Winograd, N. Lipid imaging with time-of-flight secondary ion mass spectrometry (ToF-SIMS). *Biochim Biophys Acta* **1811**, 976-990, doi:10.1016/j.bbalip.2011.05.007 (2011).
110 Malm, J., Giannaras, D., Riehle, M. O., Gadegaard, N. & Sjövall, P. Fixation and Drying Protocols for the Preparation of Cell Samples for Time-of-Flight Secondary Ion Mass Spectrometry Analysis. *Anal. Chem.* **81**, 7197–7205 (2009).

111 Nygren, H. & Malmberg, P. High resolution imaging by organic secondary ion mass spectrometry. *Trends Biotechnol* **25**, 499-504, doi:10.1016/j.tibtech.2007.07.010 (2007).
112 Nygren, H., Börner, K., Malmberg, P. & Hagenhoff, B. Localization of cholesterol in rat cerebellum with imaging TOF-SIMS. *Applied Surface Science* **252**, 6975-6981, doi:10.1016/j.apsusc.2006.02.197 (2006).
113 Borner, K. *et al.* Distribution of cholesterol and galactosylceramide in rat cerebellar white matter. *Biochim Biophys Acta* **1761**, 335-344, doi:10.1016/j.bbalip.2006.02.021 (2006).
114 Sjövall, P., Johansson, B. & Lausmaa, J. Localization of lipids in freeze-dried mouse brain sections by imaging TOF-SIMS. *Applied Surface Science* **252**, 6966-6974, doi:10.1016/j.apsusc.2006.02.126 (2006).
115 Kurczy, M. E. *et al.* Which is more important in bioimaging SIMS experiments-The sample preparation or the nature of the projectile? *Appl Surf Sci* **255**, 1298-1304, doi:10.1016/j.apsusc.2008.05.139 (2008).
116 Roddy, T. P., Cannon, D. M., Meserole, C. A., Winograd, N. & Ewing, A. G. Imaging of Freeze-Fractured Cells with in Situ Fluorescence and Time-of-Flight Secondary Ion Mass Spectrometry. *Anal.Chem.* **74**, 4011-4019 (2002).

117 Colliver, T. L. *et al.* Atomic and Molecular Imaging at the Single-Cell Level with TOF-SIMS. *Anal Chem.* **69**, 2225-2231 (1997).

118 Wittig, A. *et al.* Preparation of cells cultured on silicon wafers for mass spectrometry analysis. *Microsc. Res. Tech.* **66**, 248-258, doi:10.1002/jemt.20159 (2005).
119 Chandra, S. Challenges of biological sample preparation for SIMS imaging of elements and molecules at subcellular resolution. *Applied Surface Science* **255**, 1273-1284, doi:10.1016/j.apsusc.2008.05.073 (2008).
120 Chandra, S., Bernius, M. T. & Morrison, G. H. Intracellular Localization of Diffusible Elements in Frozen-Hydrated Biological Specimens with Ion Microscopy. *Anal. Chem.* **58**, 493-496, doi:10.1021/ac00293a053, (1986).

121 Lanekoff, I. *et al.* Time of Flight Mass Spectrometry Imaging of Samples Fractured In Situ with a Spring-Loaded Trap System. *Anal. Chem.* **82**, 6652–6659 (2010).

122 Goodwin, R. J., Pennington, S. R. & Pitt, A. R. Protein and peptides in pictures: imaging with MALDI mass spectrometry. *Proteomics* **8**, 3785-3800, doi:10.1002/pmic.200800320 (2008).
123 Woods, A. S. & Jackson, S. N. Brain Tissue Lipidomics: Direct Probing Using Matrix-assisted Laser Desorption/Ionization Mass Spectrometry. *The AAPS Journal* **8**, 391-395 (2006).

124 Yalcin, E. B. & de la Monte, S. M. Review of matrix-assisted laser desorption ionization-imaging mass spectrometry for lipid biochemical histopathology. *J Histochem Cytochem* **63**, 762-771, doi:10.1369/0022155415596202 (2015).
125 Zavalin, A., Yang, J. & Caprioli, R. Laser beam filtration for high spatial resolution MALDI imaging mass spectrometry. *J Am Soc Mass Spectrom* **24**, 1153-1156, doi:10.1007/s13361-013-0638-5 (2013).
126 Jurchen, J. C., Rubakhin, S. S. & Sweedler, J. V. MALDI-MS imaging of features smaller than the size of the laser beam. *J Am Soc Mass Spectrom* **16**, 1654-1659, doi:10.1016/j.jasms.2005.06.006 (2005).

127 Zavalin, A. *et al.* Direct imaging of single cells and tissue at sub-cellular spatial resolution using transmission geometry MALDI MS. *J Mass Spectrom* **47**, 1473–1481, doi:10.1002/jms.3132 (2012).
128 Kaletas, B. K. *et al.* Sample preparation issues for tissue imaging by imaging MS. *Proteomics* **9**, 2622-2633, doi:10.1002/pmic.200800364 (2009).
129 Schwartz, S. A., Reyzer, M. L. & Caprioli, R. M. Direct tissue analysis using matrix-assisted laser desorption/ionization mass spectrometry: practical aspects of sample preparation. *J Mass Spectrom* **38**, 699-708, doi:10.1002/jms.505 (2003).
130 Vermillion-Salsbury, R. L. & Hercules, D. M. 9-Aminoacridine As a Matrix for Negative Mode Matrix-assisted Laser Desorption/ionization. *Rapid Communication Mass Spectrometry* **16**, 1575-1581 (2002).
131 Walch, A., Rauser, S., Deininger, S. O. & Hofler, H. MALDI imaging mass spectrometry for direct tissue analysis: a new frontier for molecular histology. *Histochem Cell Biol* **130**, 421-434, doi:10.1007/s00418-008-0469-9 (2008).
132 Kaspar, S., Peukert, M., Svatos, A., Matros, A. & Mock, H. P. MALDI-imaging mass spectrometry - An emerging technique in plant biology. *Proteomics* **11**, 1840-1850, doi:10.1002/pmic.201000756 (2011).
133 Thomas, A. & Chaurand, P. Advances in tissue section preparation for MALDI imaging MS. *Bioanalysis* **6**, 967–982 (2014).

134 Angel, P. M. & Caprioli, R. M. Matrix-assisted laser desorption ionization imaging mass spectrometry: in situ molecular mapping. *Biochemistry* **52**, 3818-3828, doi:10.1021/bi301519p (2013).
135 Ye, H., Greer, T. & Li, L. Probing neuropeptide signaling at the organ and cellular domains via imaging mass spectrometry. *J Proteomics* **75**, 5014-5026, doi:10.1016/j.jprot.2012.03.015 (2012).
136 Chiang, C. K., Chen, W. T. & Chang, H. T. Nanoparticle-based mass spectrometry for the analysis of biomolecules. *Chemical Society reviews* **40**, 1269-1281 (2011).
137 Taira, S. *et al.* Nanoparticle-Assisted Laser Desorption/Ionization Based Mass Imaging with Cellular Resolution. *Anal. Chem.* **80**, 4761–4766 (2008).

138 Goto-Inoue, N. *et al.* The detection of glycosphingolipids in brain tissue sections by imaging mass spectrometry using gold nanoparticles. *J Am Soc Mass Spectrom* **21**, 1940-1943, doi:10.1016/j.jasms.2010.08.002 (2010).
139 Su, C. L. & Tseng, W. L. Gold Nanoparticles as Assisted Matrix for Determining Neutral Small Carbohydrates through Laser Desorption/Ionization Time-of-Flight Mass Spectrometry. *Analytical Chemistry*, **79**, 1626-1633 (2007).

140 Son, J., Lee, G. & Cha, S. Direct analysis of triacylglycerols from crude lipid mixtures by gold nanoparticle-assisted laser desorption/ionization mass spectrometry. *J Am Soc Mass Spectrom* **25**, 891-894, doi:10.1007/s13361-014-0844-9 (2014).
141 Chiang, C. K. *et al.* Nanomaterial-based surface-assisted laser desorption/ionization mass spectrometry of peptides and proteins. *J Am Soc Mass Spectrom* **21**, 1204-1207, doi:10.1016/j.jasms.2010.02.028 (2010).
142 Mohammadi, A. S., Fletcher, J. S., Malmberg, P. & Ewing, A. G. Gold and silver nanoparticle-assisted laser desorption ionization mass spectrometry compatible with secondary ion mass spectrometry for lipid analysis. *Surface and Interface Analysis* **46**, 379-382, doi:10.1002/sia.5609 (2014).
143 Wu, H. P., Yu, C. J., Lin, C. Y., Lin, Y. H. & Tseng, W. L. Gold nanoparticles as assisted matrices for the detection of biomolecules in a high-salt solution through laser

desorption/ionization mass spectrometry. *J Am Soc Mass Spectrom* **20**, 875-882, doi:10.1016/j.jasms.2009.01.002 (2009).
144 Belu, A. M., Graham, D. J. & Castner, D. G. Time-of-flight secondary ion mass spectrometry: techniques and applications for the characterization of biomaterial surfaces. *Biomaterials* **24**, 3635-3653 (2003).
145 Boxer, S. G., Kraft, M. L. & Weber, P. K. Advances in imaging secondary ion mass spectrometry for biological samples. *Annu Rev Biophys* **38**, 53-74, doi:10.1146/annurev.biophys.050708.133634 (2009).
146 Lockyer, N. P. Static secondary ion mass spectrometry for biological and biomedical research. *Methods Mol Biol* **369**, 543-567 (2007).

147 Sigmund, P. Sputtering by Ion Bombardment: Theoretical Concepts. *Topics in Applied Physics* **41**, 9–71 (1981).

148 Cooks, R. G. a. B., K.L. Matrix Effects, Internal Energies and MS/MS Spectra of Molecular Ion Sputtered From Surfaces. *International Journal of Mass Spectrometry Ion Physics* **53**, 111-124 (1983).
149 Vickerman, J. C. G., I. S. Surface Analysis– The Principal Techniques. *John Wiley & Sons Ltd, Chichester, UK*, 113-205,. (2009).

150 Vickerman, J. C. a. S., A.J. Secondary Ion Mass Spectrometry in Surface Analysis the Principle Technique. *John Wiley and Sons Ltd.* (1997).
151 Jones, E. A., Lockyer, N. P., Kordys, J. & Vickerman, J. C. Suppression and enhancement of secondary ion formation due to the chemical environment in static-secondary ion mass spectrometry. *J Am Soc Mass Spectrom* **18**, 1559-1567, doi:10.1016/j.jasms.2007.05.014 (2007).
152 Kötter, F. & Benninghoven, A. Secondary ion emission from polymer surfaces under Ar+, Xe+ and SF5+ ion bombardment. *Applied Surface Science* **133**, 47–57 (1998).
153 Vickerman, J. C. & Briggs, D. ToF-SIMS: Surface Analysis by Mass Spectrometry Surface Spectra, IM Publications LLP. (2001).
154 Gillen, G. *et al.* Depth profiling using C60+ SIMS—Deposition and topography development during bombardment of silicon. *Applied Surface Science* **252**, 6521-6525, doi:10.1016/j.apsusc.2006.02.234 (2006).
155 Wang, L. *et al.* High-performance transparent inorganic-organic hybrid thin-film n-type transistors. *Nat Mater* **5**, 893-900, doi:10.1038/nmat1755 (2006).
156 Chirila, A. *et al.* Potassium-induced surface modification of Cu(In,Ga)Se2 thin films for high-efficiency solar cells. *Nat Mater* **12**, 1107-1111, doi:10.1038/nmat3789 (2013).
157 Sjövall, P. *et al.* Organic Geochemical Microanalysis by Time-of-Flight Secondary Ion Mass Spectrometry (ToF-SIMS). *Geostandards and Geoanalytical Research* **32**, 267-277 (2008).

158 Jones, E. A., Lockyer, N. P. & Vickerman, J. C. Depth Profiling Brain Tissue Sections with a 40 keV C60+ Primary Ion Beam. *Analytical Chemistry*, **80**, 2125-2132 (2008).

159 Robinson, M. A., Graham, D. J. & Castner, D. G. ToF-SIMS depth profiling of cells: z-correction, 3D imaging, and sputter rate of individual NIH/3T3 fibroblasts. *Anal Chem* **84**, 4880-4885, doi:10.1021/ac300480g (2012).
160 Vickerman, J. C. & Winograd, N. SIMS—A precursor and partner to contemporary mass spectrometry. *International Journal of Mass Spectrometry* **377**, 568-579, doi:10.1016/j.ijms.2014.06.021 (2015).

161 Malherbe, J. *et al.* A New Radio Frequency Plasma Oxygen Primary Ion Source on Nano Secondary Ion Mass Spectrometry for Improved Lateral Resolution and Detection of Electropositive Elements at Single Cell Level. *Anal Chem* **88**, 7130-7136, doi:10.1021/acs.analchem.6b01153 (2016).
162 Chandra, S., Smith, D. R. & Morrison, G. H. Subcellular imaging by dynamic SIMS ion microscopy. *Anal. Chem.* **72**, 104A-114A. (2000).

163 Nunez, J., Renslow, R., Cliff, J. B., 3rd & Anderton, C. R. NanoSIMS for biological applications: Current practices and analyses. *Biointerphases* **13**, 1-26, doi:10.1116/1.4993628 (2017).
164 Pumphrey, G. M., Hanson, B. T., Chandra, S. & Madsen, E. L. Dynamic secondary ion mass spectrometry imaging of microbial populations utilizing C-labelled substrates in pure culture and in soil. *Environ Microbiol* **11**, 220-229, doi:10.1111/j.1462-2920.2008.01757.x (2009).
165 Lovric, J. *et al.* Nano Secondary Ion Mass Spectrometry Imaging of Dopamine Distribution Across Nanometer Vesicles. *ACS Nano* **11**, 3446-3455, doi:10.1021/acsnano.6b07233 (2017).
166 Chait, B. T. & Standing, K. *A time-of-flight mass spectrometer for measurement of secondary ion mass spectra*. Vol. 40 (1981).
167 Steffens, P., Niehuis, E., Friese, T., Greifendorf, D. & Benninghoven, A. A time-of-flight mass spectrometer for static SIMS applications. *Journal of Vacuum Science & Technology A: Vacuum, Surfaces, and Films* **3**, 1322-1325, doi:10.1116/1.573058 (1985).
168 Benninghoven, A. Chemical Analysis of Inorganic and Organic Surfaces and Thin Films by Static Time-of-Flight Secondary Ion Mass Spectrometry (ToF-SIMS). *Angewandte Chemie* **33**, 1023-1043 (1994).
169 Castaing, R. & 1981, G. S. Analytical microscopy by secondary ion imaging techniques. *J. Phys. E: Sci. Instrum* **14**, 1119–1127 (1981).

170 Liebl, H. Ion Microprobe Mass Analyzer. *Journal of Applied Physics* **38**, 5277-5283, doi:10.1063/1.1709314 (1967).
171 Henss, A. *et al.* Applicability of ToF-SIMS for monitoring compositional changes in bone in a long-term animal model. *J R Soc Interface* **10**, 20130332, doi:10.1098/rsif.2013.0332 (2013).
172 Seliger, R. L., Ward, J. W., Wang, V. & Kubena, R. L. A high-intensity scanning ion probe with submicrometer spot size. *Applied Physics Letters* **34**, 310-312, doi:10.1063/1.90786 (1979).
173 Prewett, P. D. & Kellogg, E. M. Liquid metal ion sources for FIB microfabricationsystems — recent advances. *Nuclear Instruments and Methods in Physics Research* **6**, 135-142 (1985).

174 Thiel, V. & Sjövall, P. Using Time-of-Flight Secondary Ion Mass Spectrometry to Study Biomarkers. *Annual Review of Earth and Planetary Sciences* **39**, 125-156, doi:10.1146/annurev-earth-040610-133525 (2011).
175 Gunnarsson, A., et al. Spatial-Resolution Limits in Mass Spectrometry Imaging of Supported Lipid Bilayers and Individual Lipid Vesicles. *Anal. Chem.* **82**, 2426–2433 (2010).

176 Gazi, E. *et al.* The combined application of FTIR microspectroscopy and ToF-SIMS imaging in the study of prostate cancer. *Faraday Discussions* **126**, 41–59, doi:10.1039/b304883g (2004).

177 Parry, S. & Winograd, N. High-Resolution TOF-SIMS Imaging of Eukaryotic Cells Preserved in a Trehalose Matrix. *Analytical Chemistry* **77**, 7950-7957 (2005).

178 Delcorte, A. & Garrison, B. J. Sputtering Polymers with Buckminsterfullerene Projectiles: A Coarse-Grain Molecular Dynamics Study. *J. Phys. Chem. C* **111**, 15312-15324 (2007).

179 Seifert, B. *et al. Integrated Electric Propulsion Systems for Small Satellites*. (2014).

180 Angerer, T. B., Blenkinsopp, P. & Fletcher, J. S. High energy gas cluster ions for organic and biological analysis by time-of-flight secondary ion mass spectrometry. *International Journal of Mass Spectrometry* **377**, 591-598, doi:10.1016/j.ijms.2014.05.015 (2015).

181 Rabbani, S., Razo, I. B., Kohn, T., Lockyer, N. P. & Vickerman, J. C. Enhancing ion yields in time-of-flight-secondary ion mass spectrometry: a comparative study of argon and water cluster primary beams. *Anal Chem* **87**, 2367-2374, doi:10.1021/ac504191m (2015).

182 Tian, H., Maciazek, D., Postawa, Z., Garrison, B. J. & Winograd, N. CO2 Cluster Ion Beam, an Alternative Projectile for Secondary Ion Mass Spectrometry. *J Am Soc Mass Spectrom* **27**, 1476-1482, doi:10.1007/s13361-016-1423-z (2016).

183 Weibel, D. *et al.* A C60 Primary Ion Beam System for Time of Flight Secondary Ion Mass Spectrometry: Its Development and Secondary Ion Yield Characteristics. *Analytical Chemistry*, **75**, 1754-1764 (2003).

184 Kersting, R., Hagenhoff, B., Kollmer, F., Möllers, R. & Niehuis, E. Influence of primary ion bombardment conditions on the emission of molecular secondary ions. *Applied Surface Science* **231-232**, 261-264, doi:10.1016/j.apsusc.2004.03.057 (2004).

185 Shard, A. G., et al. Quantitative Molecular Depth Profiling of Organic Delta-Layers by C60 Ion Sputtering and SIMS. *J. Phys. Chem. B* **112**, 2596-2605 (2008).

186 Brison, J. *et al.* ToF-SIMS imaging and depth profiling of HeLa cells treated with bromodeoxyuridine. *Surf Interface Anal* **43**, 354-357, doi:10.1002/sia.3415 (2011).

187 Mouhib, T., Delcorte, A., Poleunis, C. & Bertrand, P. C60 molecular depth profiling of bilayered polymer films using ToF-SIMS. *Surface and Interface Analysis* **43**, 175-178, doi:10.1002/sia.3539 (2011).

188 Nygren, H., Hagenhoff, B., Malmberg, P., Nilsson, M. & Richter, K. Bioimaging TOF-SIMS: High resolution 3D imaging of single cells. *Microsc. Res. Tech.* **70**, 969-974, doi:10.1002/jemt.20502 (2007).

189 Malmberg, P. *et al.* Depth profiling of cells and tissues by using C60+ and SF5+ as sputter ions. *Applied Surface Science* **255**, 926-928, doi:10.1016/j.apsusc.2008.05.071 (2008).

190 Fletcher, J. S. *et al.* TOF-SIMS Analysis Using C60. Effect of Impact Energy on Yield and Damage. *Anal. chem* **78**, 1827-1831 (2006).

191 Rabbani, S., Barber, A. M., Fletcher, J. S., Lockyer, N. P. & Vickerman, J. C. TOF-SIMS with argon gas cluster ion beams: a comparison with C60+. *Anal Chem* **83**, 3793-3800, doi:10.1021/ac200288v (2011).

192 Peresse, T. *et al.* Dual Beam Depth Profiling and Imaging with Argon and Bismuth Clusters of Prenylated Stilbenes on Glandular Trichomes of Macaranga vedeliana. *Anal Chem* **89**, 9247-9252, doi:10.1021/acs.analchem.7b02020 (2017).

193 Fletcher, J. S., Rabbani, S., Barber, A. M., Lockyer, N. P. & Vickerman, J. C. Comparison of C60and GCIB primary ion beams for the analysis of cancer cells and

tumour sections. *Surface and Interface Analysis* **45**, 273-276, doi:10.1002/sia.4874 (2013).

194 Kollmer, F. Cluster primary ion bombardment of organic materials. *Applied Surface Science* **231-232**, 153-158, doi:10.1016/j.apsusc.2004.03.101 (2004).

195 Touboul, D., Kollmer, F., Niehuis, E., Brunelle, A. & Laprevote, O. Improvement of biological time-of-flight-secondary ion mass spectrometry imaging with a bismuth cluster ion source. *J Am Soc Mass Spectrom* **16**, 1608-1618, doi:10.1016/j.jasms.2005.06.005 (2005).

196 Fletcher, J. S., Lockyer, N. P. & Vickerman, J. C. C60, Buckminsterfullerene: its impact on biological ToF-SIMS analysis. *Surf. Interface Anal.* **38**, 1393–1400, doi:10.1002/sia (2006).

197 Adriaensen, L., Vangaever, F., Lenaerts, J. & Gijbels, R. Matrix-enhanced secondary ion mass spectrometry: the influence of MALDI matrices on molecular ion yields of thin organic films. *Rapid Communications in Mass Spectrometry* **19**, 1017-1024, doi:10.1002/rcm.1881 (2005).

198 Brunelle, A., Touboul, D. & Laprevote, O. Biological tissue imaging with time-of-flight secondary ion mass spectrometry and cluster ion sources. *J Mass Spectrom* **40**, 985-999, doi:10.1002/jms.902 (2005).

199 Malmberg, P. *et al.* A new approach to measuring vitamin D in human adipose tissue using time-of-flight secondary ion mass spectrometry: a pilot study. *J Photochem Photobiol B* **138**, 295-301, doi:10.1016/j.jphotobiol.2014.06.008 (2014).

200 Tian, H., Wucher, A. & Winograd, N. Molecular imaging of biological tissue using gas cluster ions. *Surf Interface Anal* **46**, 115-117, doi:10.1002/sia.5509 (2014).

201 Wucher, A., Tian, H. & Winograd, N. A mixed cluster ion beam to enhance the ionization efficiency in molecular secondary ion mass spectrometry. *Rapid Commun Mass Spectrom* **28**, 396-400, doi:10.1002/rcm.6793 (2014).

202 Delcorte, A., Medard, N. & Bertrand, P. Organic Secondary Ion Mass Spectrometry: Sensitivity Enhancement by Gold Deposition. *Anal. chem* **74**, 4955-4968 (2002).

203 Delcorte, A. *et al.* Metal-Assisted Secondary Ion Mass Spectrometry Using Atomic (Ga+,In+) and Fullerene Projectiles. *Anal. chem* **79**, 3673-3689 (2007).

204 Delcorte, A., Bour, J., Aubriet, F., Muller, J.-F. & Bertrand, P. Sample Metallization for Performance Improvement in Desorption/Ionization of Kilodalton Molecules: Quantitative Evaluation, Imaging Secondary Ion MS, and Laser Ablation. *Anal. chem* **75**, 6875-6885 (2003).

205 Altelaar, A. F. M., et al. Gold-Enhanced Biomolecular Surface Imaging of Cells and Tissue by SIMS and MALDI Mass Spectrometry. *Anal. chem* **78**, 734-742 (2006).

206 Nygren, H., Malmberg, P., Kriegeskotte, C. & Arlinghaus, H. F. Bioimaging TOF-SIMS: localization of cholesterol in rat kidney sections. *FEBS Lett* **566**, 291-293, doi:10.1016/j.febslet.2004.04.052 (2004).

207 Wu, K. J. & Odom, R. W. Matrix-Enhanced Secondary Ion Mass Spectrometry: A Method for Molecular Analysis of Solid Surfaces. *Anal. chem.* **68**, 873-882 (1996).

208 Delcorte, A. Matrix-enhanced secondary ion mass spectrometry: The Alchemist's solution? *Applied Surface Science* **252**, 6582-6587, doi:10.1016/j.apsusc.2006.02.076 (2006).

209 Hanton, S. D. & Owens, K. G. Using MESIMS to analyze polymer MALDI matrix solubility. *Journal of the American Society for Mass Spectrometry* **16**, 1172-1180, doi:10.1016/j.jasms.2005.03.013 (2005).
210 Fitzgerald, J. J. D., Kunnath, P. & Walker, A. V. Matrix-Enhanced Secondary Ion Mass Spectrometry (ME SIMS) Using Room Temperature Ionic Liquid Matrices. *Anal. Chem.* **82**, 4413–4419, doi:10.1038/lipidmaps.2009.3 (2010).

211 Lerach, J. O., Keskin, S. & Winograd, N. Investigations Into the Interactions of a MALDI Matrix with Organic Thin Films Using C60(+) SIMS Depth Profiling. *Surf Interface Anal* **46**, 67-69, doi:10.1002/sia.5545 (2014).
212 Rabbani, S., Barber, A., Fletcher, J. S., Lockyer, N. P. & Vickerman, J. C. Enhancing secondary ion yields in time of flight-secondary ion mass spectrometry using water cluster primary beams. *Anal Chem* **85**, 5654-5658, doi:10.1021/ac4013732 (2013).
213 Svara, F. N., Kiss, A., Jaskolla, T. W., Karas, M. & Heeren, R. M. High-reactivity matrices increase the sensitivity of matrix enhanced secondary ion mass spectrometry. *Anal Chem* **83**, 8308-8313, doi:10.1021/ac202222h (2011).
214 McDonnell, L. A. *et al.* Subcellular imaging mass spectrometry of brain tissue. *J Mass Spectrom* **40**, 160-168, doi:10.1002/jms.735 (2005).
215 Heeren, R. M. A., Kükrer-Kaletaş, B., Taban, I. M., MacAleese, L. & McDonnell, L. A. Quality of surface: The influence of sample preparation on MS-based biomolecular tissue imaging with MALDI-MS and (ME-)SIMS. *Applied Surface Science* **255**, 1289-1297, doi:10.1016/j.apsusc.2008.05.243 (2008).
216 McDonnell, L. A., Heeren, R. M., de Lange, R. P. & Fletcher, I. W. Higher sensitivity secondary ion mass spectrometry of biological molecules for high resolution, chemically specific imaging. *J Am Soc Mass Spectrom* **17**, 1195-1202, doi:10.1016/j.jasms.2006.05.003 (2006).
217 Altelaar, A. F., Luxembourg, S. L., McDonnell, L. A., Piersma, S. R. & Heeren, R. M. Imaging mass spectrometry at cellular length scales. *Nat Protoc* **2**, 1185-1196, doi:10.1038/nprot.2007.117 (2007).
218 Dowlatshahi Pour, M., Malmberg, P. & Ewing, A. An investigation on the mechanism of sublimed DHB matrix on molecular ion yields in SIMS imaging of brain tissue. *Anal Bioanal Chem* **408**, 3071-3081, doi:10.1007/s00216-016-9385-3 (2016).
219 Sjövall, P., Lausmaa, J., Nygren, H., Carlsson, L. & Malmberg, P. Imaging of Membrane Lipids in Single Cells by Imprint-Imaging Time-of-Flight Secondary Ion Mass Spectrometry. *Anal. chem* **75**, 3429-3434 (2003).

220 Bletsos, I. V. *et al.* Structural Characterization of Model Polyurethanes Using Time-of-Flight Secondary Ion Mass Spectrometry. *Anal. Chem.* **61**, 2142−2149 (1989).

221 Murayama, Y., Komatsu, M., Kuge, K. & Hashimoto, H. Enhanced peptide molecular imaging using aqueous droplets. *Applied Surface Science* **252**, 6774-6776, doi:10.1016/j.apsusc.2006.02.217 (2006).
222 Brummel, C. L., Lee, I. N. W., Zhou, Y., Benkovic, S. J. & Winograd, N. A Mass Spectromtric Solution to the Address problem of Combinatorial Libraries. *Science* **264**, 399−402 (1994).
223 Komatsu, M., Murayama, Y. & Hashimoto, H. Protein fragment imaging using ink jet printing digestion technique. *Applied Surface Science* **255**, 1162-1164, doi:10.1016/j.apsusc.2008.05.262 (2008).
224 Lange, S., Malmberg, P. & Nygren, H. Binding of the VCHSKT peptide to ceramide-rich and cholesterol-rich domains of cell membranes in rat pancreatic glands. *Surface and Interface Analysis* **45**, 268-272, doi:10.1002/sia.5020 (2013).

225 Nygren, H. & Malmberg, P. High-resolution imaging and proteomics of peptide fragments by TOF-SIMS. *Proteomics* **10**, 1694-1698, doi:10.1002/pmic.200900782 (2010).
226 Graham, D. J. & Castner, D. G. Multivariate analysis of ToF-SIMS data from multicomponent systems: the why, when, and how. *Biointerphases* **7**, 1-12, doi:10.1007/s13758-012-0049-3 (2012).
227 Tyler, B. J., Rayal, G. & Castner, D. G. Multivariate analysis strategies for processing ToF-SIMS images of biomaterials. *Biomaterials* **28**, 2412-2423, doi:10.1016/j.biomaterials.2007.02.002 (2007).
228 Wold, S., Esbensen, K. & Geladi, P. Principal Component Analysis. *Chemometrics and Intelligent Laboratory Systems* **2**, 37-52 (1987).
229 Bylesjö, M. *et al.* OPLS discriminant analysis: combining the strengths of PLS-DA and SIMCA classification. *Journal of Chemometrics* **20**, 341-351, doi:10.1002/cem.1006 (2006).
230 Westerhuis, J. A., van Velzen, E. J., Hoefsloot, H. C. & Smilde, A. K. Multivariate paired data analysis: multilevel PLSDA versus OPLSDA. *Metabolomics* **6**, 119-128, doi:10.1007/s11306-009-0185-z (2010).
231 Almstrand, A. C. *et al.* TOF-SIMS analysis of exhaled particles from patients with asthma and healthy controls. *Eur Respir J* **39**, 59-66, doi:10.1183/09031936.00195610 (2012).
232 Yan, X. *et al.* Lipidomics focusing on serum polar lipids reveals species dependent stress resistance of fish under tropical storm. *Metabolomics* **8**, 299-309, doi:10.1007/s11306-011-0307-2 (2011).